Annual Reviews in Control 51 (2021) 236–253

Contents lists available at ScienceDirect

Annual Reviews in Control

journal homepage: www.elsevier.com/locate/arcontrol

Review article

A comprehensive review of hyperspectral data fusion with lidar and sar data

Sevcan Kahraman [a,*], Raphael Bacher [b]

[a] Istanbul Gelişim University, Electrical and Electronics Engineering, 34315, Istanbul, Turkey
[b] Université Grenoble Alpes, CNRS, Grenoble INP*, GIPSA-lab, 38000, Grenoble, France

ARTICLE INFO

Keywords:
hyperspectral (HS) image
Light Detection And Ranging (LiDAR)
Synthetic Aperture Radar (SAR)
multi-modal data fusion
review

ABSTRACT

With the development of remote sensing techniques, the fusion of multimodal data, particularly hyperspectral-Light Detection And Ranging (HS-LiDAR) and hyperspectral-SAR, has become an important research field in numerous application areas. Multispectral, HS, LiDAR, and Synthetic Aperture Radar (SAR) images contain detailed information about the monitored surface that are complementary to each other. Thus, data fusion methods have become a promising solution to obtain high spatial resolution remote-sensing images. The main point of this review paper is to classify hyperspectral-LiDAR and hyperspectral-SAR data fusion with approaches. Moreover, recent achievements in the fusion of hyperspectral-LiDAR and hyperspectral-SAR data are highlighted in terms of faced challenges and applications. Most frequently used data fusion datasets that include IEEE GRSS Data Fusion Contests are also described.

1. Introduction

Obtaining high spatial and high spectral resolution images is a fundamental task in many applications of remote sensing, such as ground cover classification, target recognition, environmental monitoring, etc. Recent improvements in remote sensing technology have attempted to obtain high spatial and high spectral resolution images able to provide high accuracy in the classification, change detection, and other applications. Remote sensors can be categorized in two classes: active ones such as light detection and ranging (LiDAR) and synthetic aperture radar (SAR), and passive ones (Multispectral - MS, Hyperspectral - HS). Passive sensors use natural illumination, whereas active sensors use their own illumination sources and can operate during the night and in shaded areas. These sensors provide useful information about the structure on the surface (SAR), height of the material (LiDAR), and material composition (MS, HS). Thus, HS, LiDAR, and SAR images present different characteristics of information about objects or events on the observed scene from a different viewpoint. Therefore, HS, LiDAR, and SAR images have different advantages in the classification and other applications of the urban area. However, although these valuable modules have great advantages, they have some limitations. For example, HS images can characterize the spectral and spatial characteristics of objects, which is suitable for urban land use/ land cover (LULC) classification. But it is difficult to distinguish the objects with similar spectral characteristics but different elevation information such as roof and road that are both made of concrete. Compared with HS images, LiDAR data have accurate three-dimensional information, which can classify the objects by using height information. However, as it lacks the semantic information of objects, LiDAR data have poor ability to classify the objects with similar elevation and different spectral information. For example, two roads with the same height but made of different materials. Therefore, it will greatly improve classification result by fusing the two types of data. HS data provide spectral information on different wavelengths while PolSAR data represent a scattering mechanism about the observed scene in the polarization signatures. These polarization signatures reflect the physical characteristic and geometric structure of the observed scene. This means that PolSAR data have information that may not be captured by optical images. Thus, using the complementarity of LiDAR data or SAR data with HS spectral data, the performance of HS unmixing may be improved and it provides more comprehensive interpretation for tree species mapping. In this review paper, LiDAR and SAR data have been considered as an auxiliary modalities that support HS data. Recent researches have shown the potential of combining multisource remote sensing data when dealing with the land use and land cover classification tasks. A considerable amount of literature has proved the effectiveness of joint use of

* Correspondence: Phone: +90 2124227000/255.
E-mail addresses: sekahraman@gelisim.edu.tr (S. Kahraman), raphael.bacher@gipsa-lab.grenoble-inp.fr (R. Bacher).

https://doi.org/10.1016/j.arcontrol.2021.03.003
Received 23 October 2020; Received in revised form 10 March 2021; Accepted 11 March 2021
Available online 24 March 2021

HS and LiDAR. Recently, deep learning-based methods have aroused wide attention for their capability to extract high-level features. Different features were extracted from HS and LiDAR datasets to further improve the classification performance by using DCNN. Deep learning-based features add significant complementary information to the HS data and improves the land cover classification accuracy. Compared with traditional classification methods, deep-learning-based classifiers have great potential to obtain high classification performance for mixed and complex inputs.

There are numerous literature reviews about data fusion of multimodal images. Zhang [1] reviews popular approaches of multimodal remote sensing data fusion. He also discusses challenges and future trends in terms of hierarchical classification, such as pixel/data level, feature level, and decision level. M. Dalla Mura et al. [2] present a detailed discussion about the main challenges and perspectives of multimodal data fusion. They also highlight the results of the outcomes of the Data Fusion Contests organized by the IEEE Geoscience and Remote Sensing Society from 2006 to 2014. V. V. Klemas [3] reviews recent developments in wetland remote sensing, such as change detection and wetland mapping. Q. Man et al. [4] categorize fusion approaches of HS-LiDAR images for forest biomass estimation into three classes: pixel-level, feature-level, and decision-level. They also formulate some major challenges and some future research topics. L. Gómez-Chova et al. [5] present a review of the existing schemes for multisource classification of remote-sensing images. They emphasize the recent developments that exploit the synergistic usage of signal processing and machine learning, such as kernel-based fusion, sparse methods, manifold alignment, and Markov modeling. They also show several methods for solving challenging problems in the field of remote sensing. B. Wu and S. Tang [6] present a systematic review of the geometrical fusion of remote sensing data and laser scanning data that is used for better 3D mapping in various applications. They also analyze the advantages and limitations of the methods and discuss future research directions in this area.

In this survey, our main contributions can be summarized as follows:

- This study presents a comprehensive literature overview on the data fusion of HS-LiDAR and HS-SAR images and also classifies them based on used methods. As opposed to other existing taxonomies (pixel/data level, feature level, and decision level), in this paper, we classify multimodal data fusion on remote sensing imagery in terms of the following categories: feature-based, object-based, pixel-based, geometric-based, graph-based, kernel-based, statistical-based, ensemble-based, convolutional-based, hybrid-based, and filter-based approaches. For each category, we also present the most recent references.
- In addition to providing summary tables of multimodal data fusion approaches, we also summarize significant points of each approach as a guide for future researches.
- We give a brief description of multimodalities and their features, advantages, and limitations.
- We address challenges for multimodal data fusion in remote sensing such as cloud shadow regions and we also introduce most frequently used data fusion datasets that include IEEE GRSS Data Fusion Contest Datasets.

This paper is organized as follows: in section 2, multimodalities and their features are introduced. In section 3, some application areas and challenges of multimodal data fusion are explained. Based on used approaches, the classification of data fusion of HS-LiDAR is presented in Section 4 and similarly, the classification of data fusion of HS-SAR is introduced in Section 5. Lastly, section 6 concludes this review.

2. Modalities in Remote Sensing

In remote sensing HS imaging collects and processes information from the observed scene across the electromagnetic spectrum. HS sensors reflect vast portions of the electromagnetic spectrum to the objects. In this way, HS sensors collect data across a wide range of the spectrum (VNIR-LWIR plus TIR) at small spectral resolution (5-15 nm) and high spatial resolution (1-5 m). This allows detailed spectral signatures to be identified for different imaged materials. HS imagery can be collected through different types of platforms. HS imager mounted on a fixed platform that can move or scan with a calibrated circular mechatronic rotation stage. Different remote-sensing platforms can be used to conduct environmental monitoring and surveillance in an urban environment. The dispersed energy is received by a digital camera attached to the back of the spectrograph. This process is called HS image acquisition mechanism that includes the camera synchronization. The acquisition of data is a fundamental step in all types of application areas. HSI data preprocessing step aims to achieve a denoised image with less intraclass variability and greater spatial smoothness. It is very important to know HS image data structure to be able to apply the appropriate preprocessing technique. A brief and broad overview of the main spectral preprocessing techniques, denoising, scatter correction, and derivatives must be highlighted.

2.1. Overview of Hyperspectral Data

Multimodal sources provide information about different aspects of an observed scene. For instance, HS images provide horizontal detailed spectral information about an imaged scene. Therefore, it is easy to distinguish between water, soil, or vegetation in that pixel [7]. In contrast to MS sensors, HS sensors are able to accurately discriminate similar classes [8] and land surface classification [9]. HS imaging can also identify asphalt and other road elements by using the spectral signatures of transport networks on trafficable areas [10]. However, HS images cannot distinguish different objects produced from the same material (e.g., concrete road and concrete roof). Furthermore, HS imaging suffers under cloudy weather conditions. Numerous features can be extracted from HS data, such as spectral features (spectral reflectance and spectral indexes) and spatial features (morphological features - MoAPs). The most generally used HS features are explained briefly in the following. Generally, morphological operators are applied in remote--sensing imagery to extract important information about the observed scene, such as the extraction of spatial information from the GSD normalized difference vegetation index (NDVI) and open street map (OSM) “building” images. Morphological profiles (MPs) compose of opening and closing processes with a structural element (SE), contains low-level features such as shape and size information. Attribute profile (AP) is defined as a generalization of the morphological profile and uses a series of morphological attribute filters. AP extracts the most informative features of an image such as the length, shape, and area of objects [11]. APs can also model middle-level features such as homogeneity and textures. Multivariate attribute (multi-attribute) profile (MAP) contains the area and the standard deviation as two types of attributes. Extended multi-attribute profiles (EMAPs) consist of n thinning and n thickening transformations of the related principal component (PC) with four attributes: length of diagonal of the bounding box, area, standard deviation, and moment of inertia. EMAPs also perform a multilevel decomposition of the input image and model the spatial information of the adjacent pixels by using attribute filters. AP can be applied only on a gray-scale image. To adapt the AP concept to HS image, a feature reduction technique (such as PCA) or a feature extraction (independent component analysis - ICA) approach can be performed on the HS data and EMAP that exploits the most important PCs as base images. Subsequently, APs can be applied to the first PCs. In [12], a strategy has been proposed to classify HS images in terms of spectral and spatial information with the aid of EMAP. Also, the cloud map can be revealed by using features extracted from HS ($EMAP_{shsi}$) [13]. In 2016, to extend the concept of the AP, P. Ghamisi et al. proposed extinction profiles (EPs). EPs are generated by applying several extinction filters (EFs) such as a

series of thinning and thickening transformations. In this process, threshold values are increased progressively. EPs are performed to obtain the spatial and contextual information from an HS image. It has also been shown that extinction filters perform more efficiently as compared to attribute filters remote sensing panchromatic images [14]. An extended EP (EEP) has been proposed in [15]. EEP may be obtained in two ways: either by reducing the dimensionality of the data with a generic transformation or by applying EPs on the important characteristics. These mentioned features are mostly applied to particularly the data fusion of HS-LİDAR. A more comprehensive explanation will be given in later sections.

2.2. Overview of LiDAR Data

LiDAR gives precise vertical and horizontal point cloud data, which can capture the 3D structure of the Earth's surface and geometric information (i.e., height, slope, orientation, curvature, tree height, and tree profile) in all weather conditions [16]. This geometric information gives an important knowledge for land and forestry applications. For example, to distinguish elevated features such as buildings and plants. Compared to MS and HS data, LiDAR data present several advantages. LiDAR data provide high-accuracy structural data that can be used to distinguish different classes with different heights, for instance, roads and buildings in urban areas [17, 18]. However, LiDAR cannot separate different objects that have the same altitude (e.g., a grass field and a swimming pool). Also, because of the provision of a narrow range of spectral information, the single usage of LiDAR data is limited for land-use classification [19]. It is crucial to decide which information should be extracted from the LiDAR for used application areas. There exist many LiDAR-derived features such as spatial distances, heights, canopy penetration, and elevation of the observed surface as model--driven LiDAR-derived features such as Digital Surface Model (DSM), Digital Terrain Model (DTM), Digital Elevation Model (DEM), Canopy Height Models (CHMs), and Ground Height Difference (GHD). In addition, OSM [20] can be extracted from LiDAR data for extracting site description and full-waveform LiDAR (FWL) [21] can also be derived from LiDAR data for generating ortho-waveforms to estimate shallow water bathymetry. Furthermore, elevation information (morphological features) extracted on LiDAR features can be obtained as MPs [22]. To model the elevation information from the LiDAR image, AP can also be applied. An attribute thinning performs on bright materials with high elevation in the LiDAR image, for example the top of a roof, while attribute-thickening performs on dark objects with low height in the LiDAR image, such as swimming pools. APs of LiDAR image is not effected by clouds. By using EMAP, spatial, and elevation information can be computed from LiDAR data. EPs are also performed to obtain elevation information from LiDAR.

2.3. Overview of SAR Data

SAR is an active imaging sensor and works under all weather conditions such as fog, smoke, rain, and clouds. SAR images give texture, amplitude, phase, land structure information, and features about the shape of the objects with the high radiometric and geometric resolution, which is mainly beneficial in military and forestry applications. With this characteristic, SAR provides important information that complements information provided by optical systems. Soil moisture content can be obtained from SAR data for geological applications. SAR data also give accurate timber volume information and is influenced by speckle noise that should be suppressed. However, because of speckles, the adequate usage of SAR data is not easily processed for fusing techniques between optical and SAR data. Feature normalization is a fundamental task before fusing the two multimodal data. Fusion and clustering of multimodal data are preprocessing steps for developing a forest monitoring system [23]. HS imagery cannot measure topographic mapping capabilities. Using imaging radar interferometry, the DEM data can be generated. DEM data, produced by the IFSAR measurements, yield a better detection of the earth topography. HS images also have coarser resolution than the AIRSAR data. P. Gamba and B. Houshmand [24] studied the data fusion of HS and IFSAR for 3D urban characterization. Polarimetric Synthetic Aperture Radar (PolSAR) is used to make measurements in different polarization waves.

The geometric structure of the land surface and soil moisture affects the sensitivity of SAR data. SAR images have several drawbacks such as backscatter saturation with complex stand structure, topography effect in mountainous regions, and limited data acquisition speed. Several features can be extracted from SAR image, for instance, canopy cover, timber volume, and terrain features. Polarimetric features such as 3 polarimetries (HH/HV/VV), polarimetric entropy, averaged alpha angle, anisotropy, and three scattering components can also be extracted from Phased Array type L-band Synthetic Aperture Radar (PALSAR) sensor. These features can be used for terrain characterization and camouflage net detection. The PolSAR data are used to measure forest mapping characteristics. HS data provide spectral information on different wavelengths, while PolSAR data represent a scattering mechanism about the observed scene in the polarization signatures. These polarization signatures reflect physical characteristics and the geometric structure of the observed scene [25]. This means that PolSAR data have information that may not be captured by optical images. There are some challenges in the fusion of PolSAR and HS images. For example, SAR data are acquired with slant-range geometry. However, optical images are acquired with nadir-looking geometry. When geometric features are different, the same pixels of two datasets show different ground targets at the same coordinate. ALOS PALSAR, TerraSAR-X (TSX), Radarsat-2 (RS2), Sentinel-1, and Tandem-L provide PolSAR data globally. Although SAR data have a good spatial resolution, phase information, frequency bands, and polarizations of SAR data are different for each SAR sensors. Therefore, the comparison between different papers is a difficult task. The results and optimal combination of channels are changed. In addition, the dielectric constant impacts the SAR backscatter object signals. Thus, metal objects reflect high returns. Hence, the SAR signal provides information not only from the surface roughness and geometry but also from the observed material property. There are several feature extraction methods for the PolSAR images. These are: H/A/α decomposition, Freeman decomposition, Yamaguchi decomposition, etc. In addition, PolSAR data provide polarization signatures. These signatures contain information about the geometric characteristic and physical properties of the surface.

3. Application Areas and Challenges of Multimodal Data Fusion

3.1. Application Areas of Multimodal Data Fusion

3.1.1. Classification of urban scenes

Getting information about urban land surface structure fast and accurately is also an important target for regional governments. This can allow better environmental management and better urban planning and disaster response in view of economic and ecological interest in the urban scene [26] and the expansion of the urban populations [27]. In addition, mapping of urban LULC and updating these maps are very important for environmental monitoring, telecommunication, and urban planning [28]. In practice, it is also necessary to monitor the changes in coastal wetlands for wetland protection [3]. Urban areas are usually a complex and dynamic environment and contain a challenging mosaic of different materials, which yields the confusion spectrum of objects. This complexity makes it difficult to meet all urban application requirements for a single sensor in remotely sensed data [29]. Therefore, to provide all important information about feature extraction and classification purposes, a single sensor is not enough [30]. Hence, various research studies have been carried out in urban land use classification by using HS imagery and LiDAR data fusion to improve classification performance in remote-sensing technology [31, 32, 33]. Recently, several

local climate zone classification frameworks were also proposed for making easier urban climate studies.

3.1.2. Environmental Monitoring, Treatment, and Management

Across the world, many forests are increasingly subject to fire, drought, insect outbreak, and disease due to climate change. Forest structure measurements and vegetation classification are significant research fields for numerous applications such as forest inventories. Hence, for sustainable forest management, the monitoring of forests from remote sensing data is an effective technology. Therefore, the joint usage of HS and LiDAR data for the analysis of complex environments in forest areas has been studied deeply by many researchers. The combination of HS and LiDAR data is used for the assessment and prediction of forest fire risk and fire behavior for forest fire management [34]. Forests with varying tree density and canopy cover to represent a gradient of vegetation and topography [31]. W. A. Marcus and M. A. Fonstad [32] investigate high-resolution LiDAR, HS, and MS data collected from unmanned aerial vehicles for controlling forests with varying tree density and canopy cover. Specifically, it is demonstrated that high spatial and spectral resolution data from UAVs are used to classify vegetation at the species level. MS-HS images and bathymetric LiDAR data are widely used in remote sensing technologies for this purpose [32]. In addition, forest resources are one of the most significant sinks for the global carbon cycle [6]. Furthermore, remote sensing mapping of river bathymetry is extensively used in hydrodynamic modeling. For a better understanding of fluvial processes, remote sensing images make a significant contribution to rivers for accurate quantitative water depth and bottom composition observations [33]. Z. Pan et al. [21] analyze the approach of voxelized bathymetric FWL to estimate shallow water bathymetry and turbidity. T. Matsuki et al. [35] present a framework for tree species classification using HS imagery and LiDAR-derived CHM data. Y. Du et al. [36] introduce an effective information extraction model about aboveground biomass estimation of wetland vegetation Suaeda salsa by using MS, HS, and LiDAR data. In addition, the classification of tree species in forest areas is a major challenge for forest management [37]. With the improvements of remote sensing imagery, the classification of individual tree species and the identification of individual trees [38] are the next target of the research for forestry applications. For example, the tree species, heights, site qualities, diameters at breast height, ages, and so forth. Furthermore, the estimation of stem diameters can be very helpful for forest inventory [39]. Several approaches have been developed for the fusion of both HS and LiDAR data for tree species mapping: F. M. B. Van Coillie et al. [40] use HS and LiDAR data for tree species mapping purposes. Also, T. D. Pham et al. [41] provide a comprehensive review for mapping mangrove species, assessing changes, and estimating their biomass, with summarizing the studies that have been undertaken since 2010. They also highlighted some future directions.

3.2. Challenges of Multimodal Data Fusion

Classification of HS image is a challenging task. These challenges are the high dimensionality of the feature space, the restricted number of training sample examples, the existence of mixed pixels, and a high degree of correlation between sequential feature bands [42]. These challenges bring about the necessity of extra information from other sources. There have been lots of attempts to combine complementary multisource modalities. Moreover, the fusion of multiple types of data is not an easy task [43]. Combining some of these technologies can cause some challenges such as the cloud shadow region, selecting the best subset of features, curse of dimensionality, etc.

3.2.1. Cloud Shadow Region Problem

Doing data fusion between multimodal data comes with some challenges. For instance, in view of the shortage of direct illumination, objects under shadows reflect considerably fewer photons into an HS remote optic sensor. This mainly causes lower radiance levels near to noise in the cloud shadow areas. Therefore, shadow areas are affected by the reliable classification results. HS images cannot be sufficient for detecting or classifying an object under shadows. This process can be particularly challenging [44]. Hence, cloudy regions in HS images need to be modified for accurate classification performance. There have been several attempts to perform object classification in these shadow areas [45, 46]. Moreover, because of clouds emerging and moving irregularly, it is highly unpredictable to model their action. The shadow region and extracted shadow region can be easily seen from the University of Houston campus data in Figure 1. [47];

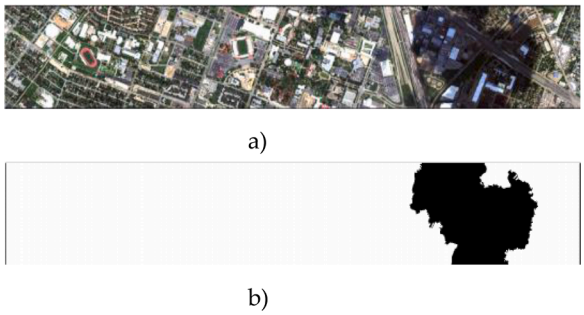

Figure 1. Shadow region on June 2012 over the University of Houston campus a) False RGB image of HS data and b) Extracted cloud shadow map [47].

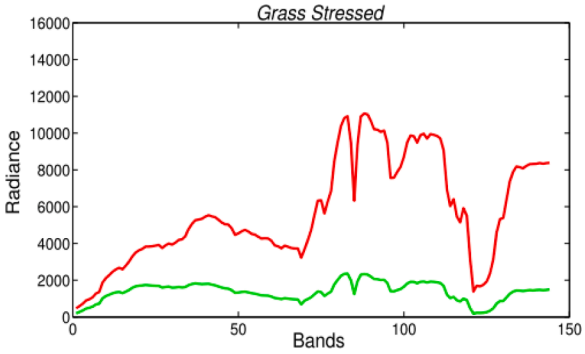

Figure 2. Shadow and nonshadow regions have different reflectance values in [47].

The spectral information under the cloud shadow region is completely different from the normal spectral signature of the sampled objects. This negatively affects the performance of the classification. For example, assume a region where there are partially occluding trees on a road. The differences in the elevation cause single pixels to have energy reflected from both the tree leaves and the road. The shade affects these pixels. This problem requires additional information resources to decrease these negative effects. Unlike HS sensors, LiDAR data can provide accurate data under almost any meteorological conditions without the requirement of any external source of illumination. Once these multimodal data are combined, it can make a supplementary effect for a more detailed interpretation of the land surface materials. The cloud-covered regions are categorized accurately by using features extracted from LiDAR data. For instance, extracted $EMAP_{slid}$ features from LiDAR data can be used for improving cloud-shadow region classification performance. Because LiDAR data cannot be influenced by the clouds. Radiances of materials in cloud shadow and noncloud shadow areas are very different from each other and can be easily seen in Figure 2. [47].

The cloud shadow region problem is a specific problem for HS-LiDAR data fusion. There are also several general problems that are related to a data fusion problem and also other kinds of data-processing problems.

Table 1
IEEE GRSS Data Fusion Contest Data Sets

Year	Sensor	Dataset	Description	Ref.
2006	QuickBird, Pléiades	MS and PAN	Focus on pansharpening	[54]
2007	ERS, Landsat	SAR and MS	Land cover urban mapping	[55]
2008	ROSIS-03	HS	Classification of HS data on urban area	[56]
2009-2010	SPOT, ERS-1	Optical and SAR	Change detection and the detection of flooded areas	[57]
2011	WorldView-2	MS, PAN, and LiDAR-DSM	Object tracking	[58]
2012	QuickBird, WorldView-2, TerraSAR-X, DigitalGlobe	MS, SAR, and LiDAR-DEM	(i) Assessing urban density by MS-LiDAR, (ii) SAR-LiDAR data for change detection and image interpretation, and (iii) surface reflectance retrievals	[59]
2013	NSF-funded Center	HS and LiDAR-DSM	Unsupervised and supervised classification	[60]
2014	LWIR, VIS	RGB data and long-wave (thermal) infrared HS	Land cover classification	[61]
2015	CISS	RGB images and 3-D LiDAR point cloud	ISO containers identification in the 3-D	[62]
2016	Deimos-2 and Iris camera	RGB images, PAN, and MS	Registration, semantic segmentation, and change detection	[63]
2017	Landsat 8, Sentinel-2, and OSM	MS and Vector data	Local climate zones classification	[64]
2018	NCALM	MS-LiDAR and HS	Urban land use and land cover classification	[65]
2019	WorldView-3 and DigitalGlobe	PAN, MS, and LiDAR	semantic 3D reconstruction and stereo using machine intelligence and deep learning, Urban Semantic 3D data	[66]

3.2.2. *The selection of the best subset of features*

A fundamental step to obtain a powerful classifier in classification is to select the discriminative features. As there are many available attributes (such as spectral, spatial, morphological, geometrical, topological, and textural features), the precise extraction of useful information is very difficult. The optimal feature subset selection should be optimized for reliable classification performance. To extract valuable features, a variety of approaches have been developed. For example, Random forests (RF) provides a natural way to select features. In addition, fused features can be used to obtain accurate classification results. Some researchers think that the fused features give better performance results in a lower dimensional subspace [48].

3.2.3. *Curse of Dimensionality*

The increase in diverse number of features may lead to a high dimensionality problem on input features. Accordingly, spectral, spatial, and elevation features from different data modalities may lead to the excessive computational time and the problem of the curse of dimensionality [49, 50]. To overcome this issue, different feature reductions [51], feature extraction [52], and feature selection approaches [53] can be performed. To address this problem, several studies have been reported in the literature. In this review, these approaches have been categorized in terms of the applied technique.

3.3. *Available Datasets*

There are numerous HS-LiDAR and HS-SAR datasets. Several HS-LiDAR data sets are Tama Forest Science Garden in Tokyo-Japan, Samford ecological research facility, Queensland-Australia, Eastern part of Brussels, San Francisco-USA, Bosco della Fontana, Po Plain Mantua-Italy, Dafeng District Yancheng, Jiangsu Province China, Italian Alps, Municipality of Pellizzano, Trento-Italy, Forested area Wijnondale-Belgium, Extremadura-Spain, Mid Atlantic region of the USA, Palm species, Washintonia, California, Gulfport Mississippi, Optech Gemini LiDAR, Oregon State University-Valley Library, Gulfport Mississippi, and Univ. of Florida. HS-SAR data sets include Downtown area Winnipeg Canada, Shimokawa Town, Hokkaido-Japon, Vicksburg Mississippi, The city of Munich-Berlin-Germany, Lobburi Nakhon, Ratchasima and Saraburi Thailand, Wilkinunich-Berlin, IKONOS Landsat & Radarsat Hyperion & HyMap AVIRS, Fontainebleau, forest South of Paris-France, Sanya region, Kjeller Norway, Radarsat-I and OMIS-I north suburb of Beijing-China, and ALOS PALSAR Vancouver Island British Columbia-Canada. HyMap HyEurope campaign DLR, TopoSys-DSMDatasets are provided by The Data Fusion Technical Committee (DFTC) of IEEE Geoscience and Remote Sensing Society are mostly used in the remote sensing data fusion community. This Society services as a multidisciplinary network for geospatial data fusion. DFTC also connects people and resources since 2006. The most frequently used datasets, provided by DFTC, are introduced in Table 1.

4. The Classification of HS-LiDAR Data Fusion

Data fusion is considered as the integration of several images into a new image using algorithms. Recently, it has become a new trend to apply multimodal data fusion in remote sensing applications. Several methods have been examined for the fusion of HS and LiDAR data for solving the problem of exploiting the information coming from multiple features. As Hossain et al. [67] said, there is no single remote sensing technology that is convenient for all remote sensing tasks. During the last decades, several researchers have performed the integration of HS and LiDAR data in different application areas such as the separation of vegetation classes, identification of tree species, forest structure analysis, shallow water bathymetry, classification of urban areas, forest fire management, above-ground biomass estimates, microclimate modeling, and fuel type mapping, etc.

Different types of multimodal data fusion approaches have been studied. The data fusion approaches of HS-LiDAR can be categorized into several subtitles. These are feature-based, object-based, pixel-based, geometric-based, graph-based, kernel-based, ensemble-based, statistical-based, convolutional-based, and hybrid-based.

4.1. *Feature-based HS-LiDAR Data Fusion*

Features are the most fundamental characteristics in image processing, including remote sensing applications. Therefore, the feature-level multimodal fusion framework is performed based on the extraction of several multimodal spectral and structural features from HS and LiDAR data. The general rationale of the feature-based multimodal data fusion approach is illustrated in Figure 4.1. Generally, a dimension reduction approach is applied to HS data, such as PCA or ICA. EAP/AP/MP is performed on a reduced image. At the same time, EAP/AP/MP is applied to LiDAR data. The obtained features are given to the SVM classifier. Figure 3 shows the general rationale of the main idea of the feature-based HS-LiDAR data fusion as a flowchart.

Next, we will consider feature-based HS-LiDAR data fusion approaches. Liao et al. [68] compare multiple-level features used for the fusion of HS-LiDAR data for classification of the urban area. They also demonstrate that approaches based on middle-level morphological

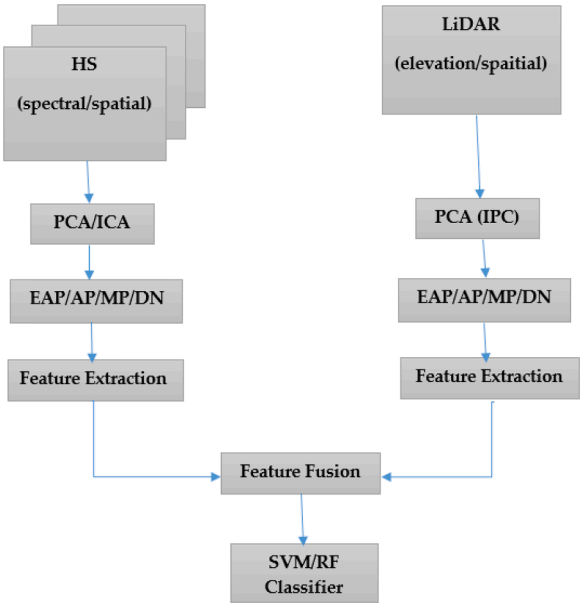

Figure 3. Flowchart of the main idea of the feature-based multimodal data fusion.

attribute features outperform methods based on high-level deep learning features. Hasani et al. [69] propose as an effective metaheuristic optimization algorithm cuckoo search for feature-level fusion strategy by using a hybrid classification system for urban area classification. M. Khodadadzadeh et al. [70] propose a multiple feature learning strategy for fusion HS and LiDAR data for urban area classification. Hence, they integrate multiple types of features obtained from HS and the LiDAR data. These data contain spectral information and different types of MPs calculated for these datasets. This method also does not require any regularization parameter. Because these different types of features could be exploited and combined, R. Luo et al. [47] propose a framework that performs HS and LiDAR data classification based on feature fusion and decision fusion by merging characterization of spectral, spatial, and elevation features for the cloudy region. The proposed method includes three steps: (1) The extraction of cloud shadow regions, (2) feature fusion of spectral and spatial information (extracted from HS image) and elevation information (extracted from LiDAR data), and 3) decision fusion of cloud shadow and noncloud shadow regions. The elevation features are used as an input for RoF classifiers. They also emphasize that cloud shadow and noncloud shadow regions have different contributions on the feature maps as per Equation (1) [13]:

$$f_{ij} = g_{ij} \times a_{ij} + \left(1 - g_{ij}\right) \times b_{ij} \tag{1}$$

This means that this framework exploits two different contributions of two classification maps. Classification is performed separately in two regions: cloud shadow regions and noncloud shadow regions, by combining spectral (obtained from HS image), spatial (obtained morphological features extracted from HS image), and elevation (obtained from morphological features extracted from LiDAR) features [47]. The final classification map is achieved by the combination of results of the cloud shadow and noncloud shadow regions. M. Pedergnana et al. [71] consider an AP for modeling the spatial information of LiDAR and HS data for the classification of urban areas by using the RF classifier. This classifier uses the features extracted from EAPs by exploiting optical and LiDAR data. F. M. B. Van Coillie et al. [40] present a feature fusion approach using different data sources in the PCA domain using HS and LiDAR data. This technique is tested for tree species mapping in forest canopy areas. This approach also uses the LiDAR height information for both the forest and tree species levels. S. Samiappan et al. [72] introduce a new fusion approach based on morphological AP and random feature selection (RFS) algorithms. They also use elevation information from the LiDAR data to resolve complex classes. F. Priem and F. Canters [73] combine HS data with LiDAR features for shadow detection in urban scenes. They used intensity-brightness thresholding with the DSM method, which is applied for shadow detection. Two datasets are used from the Eastern part of Brussels for experimental studies. These are high-resolution APEX HS imagery and a discrete waveform LiDAR data. B. Rasti et al. [74] extract spatial and elevation information from HS and LiDAR data by using EPs. Then, they fuse extracted spectral, spatial, and elevation features from HS imagery and LiDAR by using orthogonal total variation component analysis (OTVCA). OTVCA can estimate the fused features in a lower-dimensional subspace at the same time. Obtained classification maps by using OTVCA preserve the structure, because of the exploitation of TV. M. Dalponte et al. [75] propose an approach to estimate forest characteristics for the fusion of HS and airborne laser scanning (ALS) data. They also perform the estimation of both the stem volume and the stem diameter at breast height. The fusion of these data is applied for individual tree crown (ITC) levels by using the ITC delineation module and grid search strategy. HS and ALS features are combined in both the estimation and classification steps. The authors claim that with this approach, all the required parameters for a forest inventory can be estimated accurately. W. Liao et al. [76] fuse the multiscale features by modeling the local spatial information for tree species mapping on HS and LiDAR data. They generate multiscale features by considering the diameter and the height information of different tree species on multimodal data. This fuses the multiscale feature fusion that generates better tree species mapping results. X. Xu et al. [77] use a multiple morphological component analysis (MMCA) method to extract textural features in the HS data. These features are combined with the height features in the LiDAR data to get more accurate classification performance. Then, they perform a classification by using the multinomial logistic regression classifier (MLR). B. Rasti et al. [48] suggest a sparse and low-rank component analysis (SLRCA) approach for the fusion of HS and LiDAR-derived features. The approach consists of two steps: First, the extraction of spatial and elevation information from HS and LiDAR data is executed by using EPs. Second, the estimation of low-rank fused features is done by the utilization of a sparse and low-rank method. T. Matsuki et al. [35] propose a strategy that involves the combination of HS imagery and LiDAR data for individual tree classification. They also obtain spectral features of trees using PCA transformation on the HS data. The size and shape information of individual trees are acquired from the LiDAR data. Both spectral and tree-crown features are fused and used as an input SVM classifier. By using this tree-crown information and shadow correction, the classification performance is improved. The general behaviors of feature-based classification of HS-LiDAR data fusion are summarized in Table 2.

4.2. *Object-based HS-LiDAR Data Fusion*

Object-oriented classification is a developing technology that is considered as the understanding of objects versus pixels. An image object can be considered as a homogeneous set of pixels of similar spectral attributes [78]. Classification based on objects has three steps: (1) segmentation of image objects, (2) extraction of object-based scales, and (3) classification using object-oriented scales such as shape, compactness, texture, and other attributes [79]. In the object-based approach, different shape characteristics of the segmented objects are incorporated into geometrical information. In [80], LiDAR data are used for segmentation and then HS image is used to classify these segments. P. R. Marpu and S. S. Martinez [81] perform multiple-level image segmentation for the fusion of HS-LiDAR data. First, they carry out image segmentation on the extracted features from HS data. Later, information extracted from the LiDAR data is used for the classification process. Z. Zhu and C. E. Woodcock [46] investigate the object detection and classification process under shadow areas. They introduce simple

Table 2
Feature-based Classification of HS-LiDAR data fusion

Approach	Feature	Description	Datasets	Ref.	Year
Multiple kernel features	Morphological and deep learning features	Urban area classification	2013 IEEE GRSS Contest data	[68]	2017
Feature level fusion, cuckoo search, and hybrid classification	Spectral and structural features	Urban area classification	2013 IEEE GRSS Contest data	[69]	2017
Multiple feature learning	Multiple types of features	Urban area classification	2013 IEEE GRSS Contest data	[70]	2015
Multiple feature classification	AP,MAP,EAP, EMAP, and MoAPs	Classification	2013 IEEE GRSS Contest data	[47]	2017
Feature fusion and classification of features	EAPs and GLCM features	Rural area classification	Urban area of the city of Trento, Italy	[71]	2012
Feature fusion	PCA transformed features	Tree species mapping	Forest reserve Wijnondale, Belgium	[40]	2015
RFS	MAPs, area, STD, and inertia	Land cover classification	Samford ecological research facility, Queensland, Australia	[72]	2016
Shadow detection method based on LiDAR intensity brightness	Height, slope, and roughness features	Urban land cover mapping	Eastern part of Brussels	[73]	2016
OTVCA-based feature fusion	EPs	Urban area and rural region Classification	Houston-USA and Trento-Italy	[74]	2017
ITCs delineation module and grid search strategy	CHM and ALS features	Classification of tree species	Italian Alps, Municipality of Pellizzano, Trento-Italy	[75]	2014
Multiscale features fusion,	Multiscale features	Tree species mapping	Forested area Wijnondale, Belgium	[76]	2017
MMCA and MLR classifier	Textural and height features	Classification	Extremadura, Spain	[77]	2016
SLRCA and RF	EPs	Classfication	2013 IEEE GRSS Contest data, Trento-Italy	[48]	2017
Shadow correction and individual tree crown delineation	CHM, DSM, tree-crown features, size, and shape	Tree species classification	Tama Forest Science Garden, Tokyo	[35]	2015

radiance correction methods such as Tmask (multi-temporal mask) and Fmask (Function of mask) to compare spectral signatures of pixels with and without sunlight areas. A. V. Kanaev et al. [82] present a man-made target detection approach by using HS detection score localization metric in object-level to find man-made objects. First, a LiDAR sensor remotely selects objects to fit into a physical dimension. Later, the spectral signature of each object is obtained by computing the correlation score obtained with detection methods such as including the adaptive cosine/coherence estimator and the spectral matched filter (MF). M. Alonzo et al. [83] investigate the crown-object level fusion of an HS image and structural metrics extracted from the 3-D LiDAR point cloud. First, a watershed segmentation algorithm is used to delineate individual crowns from a gridded canopy maxima model. Later, spectra are extracted for each segment by using NDVI and structural metrics. After performing fusion, crowns are classified by canonical discriminant analysis. F. Leonardi et al. [84] propose a methodology that jointly employs cognitive approaches (i.e., semantic net) and data mining (i.e., genetic algorithms) for land cover urban area mapping. Height information derived from LiDAR data is used to the MS images to help the discrimination between targets with similar spectral objects.

K. Kiani et al. [85] introduce a classification strategy in an iterative Segmentation-Classification-Merging (SCM) process for object-based classification. In each iteration step, image objects are defined by using their spectral, height, and geometric characteristics. The general behaviors of object- based classification of HS-LiDAR data fusion are summarized in Table 3 above.

4.3. Pixel-based HS-LiDAR Data Fusion

Pixel-based data fusion becomes an evolving technology that is used by operating pixel by pixel. There are many pixel-based data fusion approaches. For pixel-based fusion, a fundamental pre-processing step is the spatial alignment of the LiDAR and optical data, which is known as image registration. H. Aytaylan and S. E. Yuksel [86] introduce a novel semantic segmentation approach. They simultaneously cluster and label pixels. They also introduce an MRF-based approach by combining spectral information from HS image and elevation and intensity information from the LiDAR data for improving classification results. R. Luo et al. [13] present a framework for cloudy HS and LiDAR data classification. This framework contains three steps: (1) cloud shadow extraction, (2) feature fusion between spectral, spatial (from HS), and elevation (from LiDAR) features, and (3) decision fusion of cloud and noncloud regions. Y. Liu et al. [87] propose a new spectral-spatial classification method by jointly using HS and LiDAR data. They perform data fusion in three levels: 1) the superpixel generation method is used for image partitioning, 2) for feature extraction a multimodal framework is generated, and 3) a convex framework with vectorial and superpixel-based graph total variation regularizers are performed. A. Castrodad et al. [88] suggest a sparse modeling approach by using a point cloud LiDAR and HS data for subpixel mapping and classification. They propose an unsupervised algorithm that learns a structured dictionary. This dictionary expresses each pixel as a sparse linear combination of its atoms. This provides better abundance mapping estimation.

Table 3
Object-based Classification of HS-LiDAR data fusion

Approach	Feature	Description	Datasets	Ref.	Year
Multiple level image segmentation	Spectral and spatial	Urban area classification	2013 IEEE GRSS Contest data	[81]	2015
Tmask, Fmask, and simple radiance correction method	Spectral and contextual information	Cloud, cloud shadow, and snow detection	Northeastern, United States	[46]	2014
Detection score localization metric and spectral MF	DEM	Man-made target/object detection	Mid Atlantic region of the USA	[82]	2011
Watershed segmentation, gridded canopy maxima model, and crown object level fusion	Crown and structural features	Urban tree species mapping	Palm species, Washintonia, California	[83]	2014
Genetic algorithm and cognitive approaches	DHM, DSM, DTM, spectral, geometric, topological, textural	Urban area mapping	Uberlandia city, Southeastern, Minas, Gerais, Brazil	[84]	2012
SCM	spectral, height, and geometric	Object-based classification	2013 IEEE GRSS Contest data	[85]	2014

Table 4
Pixel-based Classification of HS-LiDAR data fusion

Approach	Feature	Description	Datasets	Ref.	Year
Semantic segmentation algorithm	Fisher vector, spectral, elevation, and intensity	Classification	2013 IEEE GRSS Contest data	[86]	2016
Feature fusion and decision fusion	APs, EMAPs, DSM, spectral, spatial, and elevation	Urban area classification	2013 IEEE GRSS Contest data	[13]	2016
Superpixel-based graph total variation regularizers	APs, EAPs, and spatial	Classification	2013 IEEE GRSS Contest data	[87]	2017
Sparse modelling algorithm	Geometric and spectral	Sub-pixel mapping and classification	Gulfport Mississippi	[88]	2012
Voxelization method	FWL measurements	Preserve the characteristics of objects	Optech Gemini LiDAR	[89]	2013
Spatial regularization	DSM	Improvement abundance estimaton	2013 IEEE GRSS Contest data	[90]	2018
SLIC clustering, plane fitting technique, and LSMSVM	Geometric and colorimetric data	Segmentation an classification	Oregon State University, Valley Library	[91]	2013
FGI-HSL	Red-edge feature	Detecting man-made targets	Southern Finland, Helsinki	[92]	2015
Decision tree and machine learning algorithm	Height, elevation, spatial, size, shape, and orientation	Detect buildings	2013 IEEE GRSS Contest data	[93]	2017

H. Wang et al. [89] propose a voxelization method to use raw FWL data with HS image by the division of the waveform information into voxels. Later, they synthesize all waveforms that intersect a voxel into one 3D superposition waveform. Finally, they compare the synthesized waveform with a nadir LiDAR waveform with the voxel of interest. T. Uezato et al. [90] present a strategy that incorporates LiDAR-DSM spatial neighborhood information into HS spectral unmixing by using the spatial regularization. Results showed that the use of LiDAR data can improve the abundance estimation and robustness. Mahmoudabadi et al. [91] present an algorithm for feature extraction. They use the advantage of both colorimetric and geometric data. This approach contains three main phases: 1) a Simple Linear Iterative Clustering (SLIC) superpixel algorithm is performed for clustering and then dividing the colorimetric data, 2) a plane-fitting technique is used on each smaller cluster to obtain a set of normal vectors, and 3) the Least Squares Multi-class Support Vector Machine (LSMSVM) is used for classifying each cluster. E. Puttonen et al. [92] test The Finnish Geodetic Institute's (FGI) HS-LiDAR (HSL) system for differentiating man-made objects from natural ones by using their spectral response. They classify spatially delineated objects by using the k-nearest neighbor algorithm for each pixel spectra. They show that HS laser scanning systems have clear potential in changing lighting conditions. S. Y. Sadjadi and S. Parsian [93] perform the fusion of HS and LiDAR data at the pixel level by using a machine learning algorithm. They apply the ensemble learning method on the fused data for building extraction. They also use a sequence of classifiers and then take the average value of the obtained results to assign the label to each pixel. Thus, high accuracy in building detection is achieved.

The general behaviors of pixel-based classfication of HS-LiDAR data fusion are summarized in Table 4.

4.4. Geometric-based HS-LiDAR Data Fusion

In geometrical-based HS-LiDAR data fusion, the geometrical features are obtained through different kinds of ways before the performance of the fusion process. T. Matsuki et al. [94] propose an approach that uses HS data with morphological information of LiDAR-CHM data for tree species classification in Japanese forests. They perform star-shaped geometrical estimation on ITC delineation LiDAR-CHM data. Later, they perform classification by SVM and post-processing with a smoothing filter. J. Broadwater and A. Banerjee [95] merge standard atmospheric compensation techniques with LiDAR DSM data and Elaboration Likelihood Model (ELM) to improve reflectance estimates of HS data. They also measure scene geometry by using color image showing locations by the aid of LIDAR data. D. Lemp and U. Weidner [96] introduce an approach for the classification of roof surfaces by using geometrical and spectral segmentation. Laser scanning provides the necessary geometric information. They use geometrical segmentation with the aid of the eCognition software tool for roof surface patches. C. Dechesne et al. [97] investigate the fusion of LiDAR and MS images by using the information about the tree species obtained from MS images and geometric information obtained from 3D LiDAR point clouds data for forest segmentation and mapping. They perform the fusion in three different steps with a semantic segmentation framework: oversegmentation, classification, and regularization. The obtained results indicate that oversegmentation can be performed either on LiDAR or optical images for better classification results. The general behaviors of geometric-based classification of HS-LiDAR data fusion are summarized in Table 5.

4.5. Graph-based HS-LiDAR Data Fusion

To obtain better clustering performance, the similarity relationship between pixels can be described by using graphs. The similarity between two vertices can be defined by using a single similarity function. This function can be fed different features extracted from images. There are some graph-based multimodal data fusion studies in the literature. W. Liao et al. [98] propose a generalized version of a graph-based feature fusion method for the classification process. In this fusion method, they use spectral, spatial, and elevation information to better model the

Table 5
Geometric-based Classification of HS-LiDAR data fusion

Approach	Feature	Description	Datasets	Ref.	Year
Shadow correction and individual tree crown delineation	CHM, spectral, and morphological information	Tree species classification	Tama Forest Science Garden in Tokyo, Japan	[94]	2014
3D model are combined with ELM	Geometric properties (line-of-side) and DSM	Atmospheric compensation	Gulfport Mississippi, Univ. of Florida	[95]	2013
Geometric segmentation using eCognition software	Geometry, slope, exposition, size, DSM, and spectral	Urban roof surface classification	HyMap HyEurope campaign DLR, TopoSys-DSM	[96]	2005
Semantic segmentation, classification, and regularization	Geometric features-LiDAR ponit cloud DSM	Forest inventory and mapping	Forest in the east of France, Optech	[97]	2017

Table 6
Graph-based Classification of HS-LiDAR data fusion

Approach	Feature	Description	Datasets	Ref.	Year
Generalized graph-based fusion method	MPs, spectral, spatial, and elevation characteristics	Classification	2013 IEEE GRSS Contest data	[98]	2015
Graph-based feature fusion	MPs and spectral	Classification	2013 IEEE GRSS Contest data	[99]	2014
Semi-supervised graph-based fusion framework	MPs and spectral information	Classification	2013 IEEE GRSS Contest data	[100]	2015

actual similarity of the connected nodes in multimodal data. They also applied a graph-based feature fusion method and decision fusion method on the same datasets for better classification accuracies [99] W. Liao et al. [100] present a semi-supervised graph-based fusion by using the morphological features from HS and LiDAR data for classification. They project the spatial, spectral, and elevation features onto a lower subspace through a semi-supervised graph-based feature fusion procedure. The obtained results show improvement of the classification. The general behaviors of graph-based classification of HS-LiDAR data fusion are summarized in Table 6.

4.6. Kernel-based HS-LiDAR Data Fusion

The kernel fusion framework has been used to solve the classification problems in multisource data fusion. There are several studies about kernel-based multimodal data fusion. M. Khodadadzadeh et al. [101] propose a generalized composite kernel strategy for the fusion of HS and LiDAR data for classification purposes over a rural area in Extremadura, Spain. To carry out fusion, first, they extract morphological features from the LiDAR intensity image. Then, these LiDAR-derived feature vectors and the spectral vectors derived from HS imagery are integrated with each other in a generalized composite kernel structure. The results of multinomial logistic regression generalized composite kernel (MLR-GCK) results outperform the results of SVM classifier. P. Ghamisi et al. [102] derive a multisensor composite kernel (MCK) approach by using extreme learning machine to fuse the complementary information of HS and LiDAR data. Then, they propose a feature fusion strategy named HS Stein's unbiased risk estimator (HySURE)-MCKs . They use EPs to obtain spatial and elevation information from HS and LiDAR data, respectively. Moreover, they also use HySURE to extract the subspace spectral, spatial, and elevation features. Finally, the obtained features are used as an input to the MCK to extract the final classification map. Y. Gu et al. [103] present a multiple-kernel learning (MKL) model by integrating heterogeneous features (HF-MKL) from HS spectral images and LiDAR data for urban classification. They integrate multiscale kernels with different features by using a linear combination strategy and then perform the optimization between this kernel and conventional to obtain a better classifier. The general behaviors of kernel-based classification of HS-LiDAR data fusion are summarized in Table 7.

4.7. Statistical-based HS-LiDAR Data Fusion

Different kinds of statistical approaches have been employed for fusing HS and LiDAR data. We will now give a literature survey about statistical-based HS-LiDAR data fusion approaches. L. Ni et al. [104] propose an edge-constrained Markov random field (EC-MRF) procedure for urban area land cover classification. They use HS and LiDAR data for pixel-wise classification. They also use MRF for spatial regularization. EC-MRF approach controls the smoothness and preserves the class boundaries. Results obtained with the EC-MRF approach show highly accurate spectral–spatial classification results. B. Abbasi et al. [105] extract features and then Maximum Likelihood (ML) classifiers are performed independently on both HS and LiDAR data. Finally, a decision fusion method is applied to obtain better classification results. M. Dalponte et al. [106] use Gaussian maximum likelihood (GML) with leave-one-out-covariance algorithm (GML-LOOC) for complex forest area classification. The proposed system provides effective classification results with high accuracy in complex forest classes. H. Wu and S. Prasad [107] employ a decision fusion system based on logarithmic opinion pools (LOGP) by using an infinite Gaussian mixture model (IGMM) based classifier (IGMM-LOGP) for accurate geospatial image classification. The general behaviors of statistical-based classification of HS-LiDAR data fusion are summarized in Table 8.

4.8. Ensemble-based HS-LiDAR Data Fusion

In recent years, the ensemble method is a very popular approach for image classification. This method does not apply to one particular classifier. Instead, a series of classifiers are used, before the results' average is used to assign the label of a pixel. What follows is a literature

Table 7
Kernel-based Classification of HS-LiDAR data fusion

Approach	Feature	Description	Datasets	Ref.	Year
MLR-based generalized composite kernel and MLR-GCK	Spectral, spatial, height, morphological features, and intensity	Classification	Extremadura, Spain	[101]	2015
MCKs, KELM-CK, and HySURE-MCKs	EPs, DSM, and spectral	Complex scene classification	Houston Univ., Trento Italy	[102]	2019
HF-MKL feature fusion	HF, elevation, MPs, and NDSM	Urban classification	San Francisco-USA, 2012 IEEE GRSS Contest data	[103]	2015

Table 8
Statistical-based Classification of HS-LiDAR data fusion

Approach	Feature	Description	Datasets	Ref.	Year
EC-MRF	DSM	Urban area land cover classification	2013 IEEE GRSS Contest data	[104]	2015
Texture feature extraction on GLCM, minimum noise fraction dimension reduction, and ML classification	Geometric information, elevation, and spectral	Classification in urban areas	2013 IEEE GRSS Contest data	[105]	2015
GML-LOOC	Elevation, intensity, and DTM	Classification of complex forest areas	Bosco della Fontana, Po Plain Mantua, Italy	[106]	2008
Decision fusion and IGMM-LOGP	Statistical, geometric, and structure	Geospatial image classification	2013 IEEE GRSS Contest data	[107]	2013

Table 9
Ensemble-based Classification of HS-LiDAR data fusion

Approach	Feature	Description	Datasets	Ref.	Year
RF classifer, GBM ensemble-based classifier, and CNN	DSM, DEM, NDVI, and morphological texture contrast (MTC)	Urban land cover classification	2018 IEEE GRSS Contest data	[108]	2018
CNN, RF, and GBM	Spatial, NDI, NDMI, OSM, AVI, MNF, and SI	Local climate zone classification	2017 IEEE GRSS Contest data	[109]	2017
PC analysis, linearity preserving projection, and unsupervised graph fusion	DSM, morphological, spatial, and elevation	Classification	2013 IEEE GRSS Contest data	[110]	2018
Canonical correlation and rotation forest	DEM, DSM, CHM, Spectral, and structural	Wetland vegetation classification	Dafeng District Yancheng, Jiangsu Province China	[36]	2019

survey about ensemble-based HS-LiDAR data fusion approaches. S. Sukhanov et al. [108] present an ensemble-based approach based on MS, LiDAR, HS, and RGB imagery for urban land use and land cover classification. This approach contains Random Forest (RF) and Gradient Boosting Machines (GBM) classifiers and Convolutional Neural Networks (CNNs). Sukhanov et al. [109] apply the same technique in [108] for automatic local climate zones classification, the fusion of MS images from Landsat-8, and Sentinel-2 satellites with site description extracted from OpenStreetMap layers from LiDAR data. J. Xia et al. [110] propose a novel ensemble classifier using morphological features for HS and LiDAR data. This ensemble classifier includes PCA, linearity preserving projection, and unsupervised graph fusion methods. Experimental results show that the proposed ensemble classifier approach is effective. Y. Du et al. [36] suggest a new approach to classify the local climate zones based on ensemble learning methods on Landsat-8 data and open street map data. They extract spectral-spatial features, such as spectral indexes, morphological profiles, and spectral reflectance. For the classification steps, Rotation Forests and Canonical Correlation Forests are used. This technique reaches a relatively reliable accuracy. Table 9 summarizes ensemble-based classification of HS-LiDAR data fusion.

4.9. Convolutional-based HS-LiDAR Data Fusion

Since the last decades, traditional classification techniques such as SVM and RF classifiers used in several ensemble approaches have been changed by more sophisticated architectures of Neural Networks allowing one to consider different aspects of multimodal data. Recently, deep learning-based methods have aroused wide attention for their capability to extract high-level features. There exist some studies about convolutional-based HS-LiDAR data fusion. M. Salman ve S.E. Yüksel [111] extract MP maps from the HS and LiDAR images. Then, they integrate HS spectral data and MP with each other. They filter elevation information from LiDAR data by using the filters in the first convolution layer of AlexNet, which has a highly efficient deep convolutional architecture in image processing. P. Ghamisi et al. [112] develop the deep CNN with logistic regression. They use EPs and deep learning to fusion features extracted from HS and LiDAR data for the classification of land cover classes. Y. Chen et al. [113] present a new feature fusion strategy using a deep neural network (DNN). They use the 3D CNN for extracting the spectral-spatial features from HS data and a deep 2D CNN for extracting the altitude features of LiDAR data. Finally, they apply logistic regression to generate the final classification map. J. Xia et al. [114] introduce a fusion strategy by using Deep Forest (DF) classifier on HS and LiDAR datasets with morphological features. DF has more advantages such as achieving better results with shorter computational time than deep neural networks. Moreover, DF classifier has fewer parameters to be set. Experimental results show that the DF can achieve better classification results. Compared with traditional classification methods, deep learning-based classifiers have great potential to obtain high classification performance for mixed and complex inputs. There are several deep fusion methods in the literature that integrate multisensor data for classification, with significant improvements over current deep feature fusion architecture. These deep fusion methods confirm that combining HS and LiDAR data has significantly improved the classification accuracy using CNN features [140-145], deep NETs [142], fully convolutional networks [145], based on Dual-Branch CNN [141], and high-level deep learning features [140]. The classification performance of CNNs increases when HSI and LiDAR data are combined at the pixel level [143]. With the graph-based fusion method, deep learning fusion gets much better classification accuracies than raw data fusion. In all those works, the use of LiDAR along with optical data leads to better results with respect to classification accuracies, and it indicates that the CNN is an efficient tool for the fusion of LiDAR and HS data.

The general behaviors of convolutional-based classification of HS-LiDAR data fusion are summarized in Table 10.

4.10. Hybrid-based HS-LiDAR Data Fusion

The hybrid-based multimodal data fusion approach uses more approaches in a combined usage at the same time. For example, pixel-based and feature-based approaches. The pixel and object-based classifiers are used by Q. Mana et al. [115] for urban land use classification. In their work, maximum likelihood classification (MLC), the SVM, and object-based classifiers are applied for the classification of LiDAR and HS imagery. Their derived features such as the normalized digital surface model (nDSM), NDVI, and texture measures are also used. The obtained results demonstrate that the combination of LiDAR nDSM, intensity data, and HS data with combined pixel- and object-based classification gives better land use classification performance.

The general behaviors of hybrid-based classification of HS-LiDAR data fusion are summarized in Table 11.

Table 10
Convolutional-based Classification of HS-LiDAR data fusion

Approach	Feature	Description	Datasets	Ref.	Year
Deep convolutional architecture	MPs and EMAPs	Classification and semantic segmentation	2013 IEEE GRSS Contest data	[111]	2018
Deep learning, graph-based feature fusion, and CNN with logistic regression	MP, EPs, APs, EMEP, MEP, and DSM	Classification	2013 IEEE GRSS Contest data, Trento Italy	[112]	2017
DNN, 3D-CNN, and logistic regression	Elevation, spectral, spatial, and invariant features	Classification	2013 IEEE GRSS Contest data	[113]	2016
Deep learning classifier method and DF classifier	DSM, CHM, morphological, spatial, and elevation features	Classification	Tama forest, Tokyo, Japan	[114]	2018

Table 11
Hybrid-based Classification of HS-LiDAR data fusion

Approach	Feature	Description	Datasets	Ref.	Year
Pixel and object-based classifiers and MLC	DSM, DEM, intensity, height,spatial, nDSM, NDVI, and texture measures	Urban land use classification	2013 IEEE GRSS Contest data	[115]	2015

4.11. Filter-based HS-LiDAR Data Fusion

C. Demirkesen et al. [116] present a multimodal architecture by separation of the region shadow and nonshadow areas, respectively. They use polynomial fitting-based DEM feature extraction approach. They implement a filter for deriving shadow invariant features from a pixel spectrum in one dimension. They also use height profile evaluation techniques and context-based correction for post-processing steps. The general behaviors of filter-based classification of HS-LiDAR data fusion are summarized in Table 12.

5. The Classification of HS-SAR Data Fusion

Different types of multimodal data fusion approaches have been studied about HS and PolSAR data. A. S. P. Bhogall et. al. [117] present a study that assesses forest attribute determination by using HS-SAR data fusion over the Greater Victoria Watershed District test site on Vancouver Island, BC, Canada. To identify spatially homogeneous objects, they use segmentation techniques to measure the forest attributes. They also compute forest biomass by using MS, HS, and SAR data sets.

The data fusion approaches of HS-SAR can be categorized into several subtitles. These are feature-based, object-based, pixel-based, kernel-based, convolutional-based, and filter-based approaches. A graphical representation of the general rationale of the HS-SAR multimodal data fusion approach is illustrated in Figure 5.1. Generally, band selection/transformation/segmentation/ Normalized cut (NCUT) can be applied to HS data and segmentation/NCUT can be performed to SAR data, simultaneously. Later, these results are combined and are given as an input to SVM/RF classifier. We can see the most frequently used classifiers for HS-SAR data fusion i.e., the minimum distance (MD), a support vector machine (SVM), ML, and artificial neural network (ANN) classifiers.

Feature normalization is an important step before fusing the datasets. As optical and SAR sensors have different imaging mechanisms, most of the normalization techniques are not favorable for optical and SAR data fusion. H. Zhang et al. [118] investigate the effects of feature normalization during the data fusion process on the LULC classification between optical and SAR data. They use MD, ML, ANN, and SVM methods for comparison. They conclude that feature normalization has no influence on the results when using these classifiers. All proposed approaches have tried to overcome some difficulties by using correlation or dependencies between two sensor data. In this part of this review paper, HS-SAR Data Fusion approaches are categorized in terms of their utilized methods. The main idea of the HS-SAR data fusion is introduced as a flowchart in Figure 4. Spectral/spatial information obtained from HS data and structural/textural information can be extracted from PolSAR data, respectively. Later, band selection/transformation/segmentation/NCUT could be applied to HS data and segmentation/NCUT could be applied to PolSAR data on these feature-extracted images, respectively. Finally, SVN/RF/MD classifier can be applied to obtain a fused image.

5.1. Feature-based HS-SAR Data Fusion

Features extracted from multiple modalities can provide complementary information. SAR and MS have potential synergies, because they give complementary information about the Earth's surface. While MS gives chemical characteristic information of materials, SAR sensors provide scattering properties of the objects in the observed scene. Hence, image fusion is a very effective process to remove individual sensor limitations [119]. Multisensor remotely sensed imagery is a very powerful data for the extraction of forest feature information. In the feature-level data fusion, noise can be avoided by using the feature extraction approaches. For example, feature extraction double nearest proportion can be applied for noise reduction [120]. There are several studies about HS-SAR feature-based data fusion in the literature. T. Li et al. [121] propose a fusion approach with a synergic use of HS and PolSAR data. They use parallel feature fusion combination strategy by combining the feature-level fusion and decision-level fusion. The feature fusion classification technique relies on a parallel feature combination, while the decision level classification depends on the fuzzy set theory. Experimental results demonstrate that the proposed synergic method has better classification performance results. K. Yoshida et al. [122] implement forest monitoring schemes using HS images and PALSAR observations. They use two sparse regularization techniques to estimate species. These are sparse discrimination analysis (SDA) and LASSO regression analysis. The features, such as canopy cover, timber volume, and the height of trees are extracted from PALSAR. Later, these features

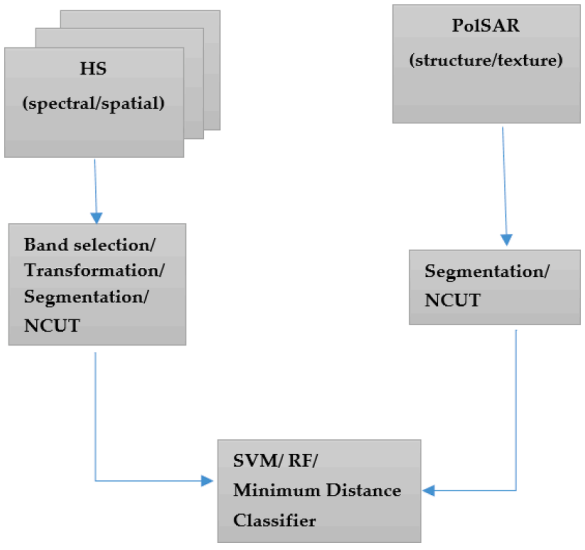

Figure 4. Flowchart of the main idea of the HS-SAR data fusion.

Table 12
Filter-based Classification of HS-LiDAR data fusion

Approach	Feature	Description	Datasets	Ref.	Year
Multimodal architecture and polynomial fitting-based DEM feature extraction	DEM shadow invariant 1-D feature NDWI, DSM, DTM, slope, curvature, and polinomial surface fitting-based features	Land cover and land use classification	2013 IEEE GRSS Contest data	[116]	2014

Table 13
Feature-based Classification of HS-SAR data fusion

Approach	Feature	Description	Datasets	Ref.	Year
Feature and decision level fusion and parallel feature combination strategy	Polarimetric features and HS features	Classification	Downtown area Winnipeg Canada	[121]	2013
SDA and LASSO regression	Tree height, canopy cover, timber volume, 3 polarimetries, and HH/HV/VV	Forest management	Shimokawa Town, Hokkaido, Japon	[122]	2011
Feature and decision-level fusion	Vegetation terrain, slope, hydrology, transportation networks, and DEMs	Trafficability assesment	HyMap and NASA Jet Propulsion Lab.	[10]	2006
PC for dimension reduction and feature extraction	Eigenvalues, eigenvectors, and terrain features	Terrain mapping and camouflage net detection	Vicksburg Mississippi	[123]	1999
Feature fusion and Dempster-Shafer evidence theory	Textural and fusion features	Land use mapping	Indian-Head Saskatchewan	[124]	2004

Table 14
Object-based Classification of HS-SAR data fusion

Approach	Feature	Description	Datasets	Ref.	Year
Segmentation by using NCUT	HH/HV features and derived probability features	Land use classification	The city of Munich, Germany	[125]	2016
Segmentation, feature selection, and rule-based classification	Material structure and dwelling density	Dwelling detection in refugee camps	AI Zaatari refugee camps, Jordan, Syria	[126]	2017

are combined and are given as an input to the sparse regularization machine learning technique. The obtained results demonstrate that sparse regularization can predict forest conditions with better accuracy. P. Chouinard et al. [10] investigate the trafficability areas in terms of the complementary nature of SAR and HS data. They perform fusion at the feature and decision levels to decide the trafficability areas. Su M. Hsu et al. [123] apply PCA on HS data to perform spectral dimension reduction and feature extraction for terrain characterization and camouflage net detection in the forest background. HS-SAR fusion is achieved with a coregistration of the images using references and a significant reduction of SAR false alarms is obtained.

A. Jouan and L. M. Canada [124] introduce the synergistic feature fusion between SAR and HS imagery for land use mapping. This data fusion module integrates PolSAR and HS data using the evidence theory suggested by Dempster-Shafer. They indicate that this synergistic fusion improves the description of land cover. The general behaviors of feature-based classification of HS-SAR data fusion are summarized in Table 13.

5.2. Object-based HS-SAR Data Fusion

Discriminatory object information could be obtained from SAR images features. Object-level multimodal data fusion approaches based on optical and SAR data provide novel aspects for the automated detection of different kinds of materials. There are some literature studies about object-based HS-SAR data fusion. J. Hu et al. [125] present an object-based fusion approach for the joint use of PolSAR and HS imagery for land use classification. They perform the extraction of features from both datasets based on an object level. This approach overcomes the geometrical mismatch problem between these two complementary datasets. Experimental results show that this approach uses scattering information of PolSAR and spectral information of HS image efficiently. K. Spröhnle et al. [126] investigate the automatic detection of dwelling types in a refugee camp through object-based image analysis technique by using very high spatial resolution optical WorldView-2 and single--polarized TSX SAR satellite data. As SAR data give an efficient characteristic for the detection of metal sheet housings, they use this property efficiently. First, they examine independently the optical data and SAR data and then they perform fusion by applying two steps: 1) the detection of optical- and SAR-based dwelling is performed with an overlay operation-based approach and 2) a feature-based analysis approach is performed.

The general behaviors of object-based classification of HS-SAR data fusion are summarized in Table 14.

5.3. Pixel-based HS-SAR Data Fusion

In pixel-based image fusion methods, image pixels are combined directly to get enhanced spatial-spectral information [127]. Generally, the pixel-level data fusion approach is not appropriate for SAR data because of the speckle noise. It requires high computational cost. C. Sukawattanavijit et al. [128] perform the GA-SVM algorithm for the fusion of multiple image modalities at a pixel level. In this approach, the genetic algorithm and SVM classifier are used for labeling the data. They classify multifrequency RS2 SAR images and Thaichote (THEOS) MS images. The experimental results demonstrate that the GA-SVM approach gives better performance results than that of the grid search algorithm. L. Dabbiru et al. [129] apply the pixel-level fusion approaches on polarimetric radar and HS images to examine the advantages of fusion for advanced classification of coastal vegetation contaminated by oil. Then they use the SVM classification algorithm with the gray-level co-occurrence matrix features. The multisensor fusion strategy with an overall accuracy of the fused feature set shows better classification performance results. The general behaviors of pixel-based classification of HS-SAR data fusion are summarized in Table 15.

5.4. Kernel-based HS-SAR Data Fusion

N.M. Nasrabadi [130, 131] implement a new nonlinear joint fusion and detection algorithm for locating anomalies from SAR and HS sensor data by using the kernel RX algorithm. In this approach, they exploit nonlinear correlation or dependencies between the two sensors to simultaneously fuse and detect the mines. As an anomaly detector, the

Table 15
Pixel-based Classification of HS-SAR data fusion

Approach	Feature	Description	Datasets	Ref.	Year
GA-SVM Algorithm and PCA	Regularization parameter C and width of kernel	Land cover classification	Lobburi Nakhon, Ratchasima and Saraburi Thailand	[128]	2017
PCA-SVM and pixel-level fusion	GLCM features, 3 band (HH/HV/VV), entropy, inertia, and variance	Analyzing the impact of the oil spill	Wilkinson Bay Louisiana Gulf of Mexico	[129]	2015

Table 16
Kernel-based Classification of HS-SAR data fusion

Approach	Feature	Description	Datasets	Ref.	Year
Kernel RX-anomaly detector	Mean and covariance	Mines detection	HS-SAR mine image	[130-131]	2008

RX algorithm is extended to investigate fusion and detection at the pixel level. Therefore, they perform the fusion nonlinearly for the detection of surface and buried mines. The general behaviors of kernel-based classification of HS-SAR data fusion are summarized in Table 16.

5.5. Convolutional-based HS-SAR Data Fusion

R. Fernandez-Beltran et al. [127] investigate the application of probabilistic latent semantic analysis (pLSA) and latent Dirichlet allocation to SAR and MS data for land cover categorization. They perform pLSA-based approach to use feature patterns from SAR and MS data for fusing. In that way, they perform an effective fusion of MS and SAR data in the land cover categorization field. R. Fernandez-Beltran et al. [132] introduce a hierarchical multimodal probabilistic latent semantic analysis (HMpLSA) techique for fusing SAR and MS data for unsupervised land cover categorization tasks. In this model, they use the advantage of two different modalities in terms of semantic patterns. They show that pLSA-based models provide better land cover categorization results than LDA. J. Hu et al. [133] use a two-stream deep CNN to combine spectrum information of the HS imagery and the scattering mechanisms of PolSAR data for urban classification. These are feature extraction and feature fusion steps. They fuse the feature maps of the HS image and the PolSAR stream. Furthermore, they apply for the first time, a deep CNN for the fusion of HS imagery and SAR data. Hence, they obtain higher classification accuracy. M. Chiarella et al. [134] implement the effectiveness of the Neural Fusion toolset for the remote sensing aided feature extraction (AFE). They also summarize the approaches used in Neural Fusion to create its deep files. In this way, pattern learning and recognition is performed. Thus, they demonstrate that Neural Fusion can ingest multiple layers and can discover salient features for utilizing image mining. E. Volden et al. [135] investigate the classification of forest areas by fusing SAR data and spectrometer. They employ a GML classifier. Combining two data sets by using GML gives good performance results. Also, the possibility to use the amplitude of polarimetric features for land cover mapping is investigated. W. Xianghai et al. [136] present an algorithm based on sparse representation and an adaptive neural network in the nonsubsample shearlet transform space for SAR and MS image pansharpening. This approach is specific to region orientation features in the high-frequency subband. They also suggest an adaptive pulse coupled neural network (PCNN) analysis model. Therefore, the algorithm gives a better spatial resolution of the MS image. By the way, the spectral information of the fusion image is also guaranteed. A. H. S. Solberg et al. [137] introduce a new method based on a Bayesian formulation for the fusion of remotely sensed MS image and SAR data. Their fusion model improves the classification error rates when it is compared to the single-source classifiers. They reduce the error rate from 33% to 22% fusion of SAR and MS images from different dates. They achieve only minor improvements in the classification error rates when fusing a SAR and MS image captured at the same date.

The general behaviors of convolutional-based classification of HS-SAR data fusion are summarized in Table 17.

5.6. Filter-based HS-SAR Data Fusion

Q. Zhou et al. [138] proposed a speckle reduction appoach for HS and SAR image fusion. They combine the coherent portions from minimum noise fraction (MNF) transformation for HS image and the SAR image. They use the Correlation Simulating Analysis Model (CSAM) to smooth the image. Therefore, they present a speckle reduction approach that relies on HS and SAR image fusion. Experimental results demonstrate that the presented model in this paper smoothes the noise and keeps both the features well. D. G. Goodenough et al. [139] investigate integration and fusion approaches of polarimetric SAR, HS, and LiDAR data for the extraction of useful forest information. With this study, they emphasize the usage of fully polarimetric SAR to perform land cover classifications and forest change monitoring. The general behaviors of

Table 17
Convolutional-based Classification of HS-SAR data fusion

Approach	Feature	Description	Datasets	Ref.	Year
pLSA-based image fusion and LDA	Optical features based on gray-level cooccurence matrix and polarimetric	Land cover categorization	Munich, Berlin, Germany	[127]	2018
HMpLSA	Correlation semantic and local-primitive	Land cover categorization tasks	Wilkinunich, Berlin, Roma	[132]	2018
Deep CNN for extracting features	HH/HV, entropy, mean, and eigenvalue	Urban scene classification	Munich, Germany	[133]	2017
Neural Fusion methods for AFE	Context, contour, periodic textures, gray-scale variance, and curvature	Image mining	IKONOS, Landsat & Radarsat Hyperion & HyMap AVIRS	[134]	2003
GML classifier	Mean, HH/VV polarization	Classification of forest and discrimination of tree species	Fontainebleau, forest, South of Paris, France	[135]	1998
Adaptive NN and sparse representation and PCNN	NSST and high frequency subband coefficient, geometric texture information,	pansharpening	Sanya region	[136]	2018
Bayesian Formulation	feature vector, and textural features	Land use classification	Kjeller Norway	[137]	1994

Table 18
Filter-based Classification of HS-SAR data fusion

Approach	Feature	Description	Datasets	Ref.	Year
MNF transformation and CSAM	Radiometric, textural, covariance, and eigenvalue	Speckle reduction method	Radarsat-I and OMIS-I north suburb of Beijing, China	[138]	2010
Jong-Sen Lee Algorithm, Shane Cloude Decomposition	Quad-pol feature, DEM, DSM, DCM, stem density, crown-closure, and height	Forest information extraction	ALOS PALSAR Vancouver Island British Columbia, Canada	[139]	2008

Table 19
Synthesize table for HS-LiDAR data fusion

Method	Tackled Problem	Features	Approach	Ref.
Feature	Urban-area classfication and tree species mapping	Morphological, deep learning, spectral, structural, spatial, elevation, AP, MAP, EAP, EMAP, MoAPs, GLCM, PCA transformed features, height, size, shape, slope, roughness, and CHM	Feature fusion, decision fusion, cuckoo search, Hybrid classification, multiple feature learning, RFS, OTVCA, ITCs,Grid search, MCA, MLR, and SLRCA	[35,40,47, 48,68-77]
Object	Urban-area classfication, tree species mapping, snow, and target and object detection	Spatial, spectral, structural, topological, textural, contextual, geometric, DEM, DHM, DSM, DTM, individual crown object scale, and height	Hierarchical image segmentation, TMask, FMask, Score Localization metric, spectral matched filter, watershed segmentation algorithm, genetic algorithm, and SCM	[46, 81-85]
Pixel	Urban-area classification, sub pixel mapping, and detect buildings	Fisher vectors, spectral, apatial, elevation, height, orientation, geometric, intensity, EMAPs, EAPs, DSM, FWL measurements, and red edge feature	Semantic segmentation, Feature fusion, decision fusion, superpixel generation method, sparse modelling, voxelization method, SLIC clustering, and LSMSVM	[13, 86-93]
Geometric	Tree species and urban roof surface classification, atmospheric compensation, forest inventory, and mapping	CHM, spectral, morphological, geometric, DSM, slope, expostion, size, and surface materials	Shadow correction, individual tree crown delineation, IPF, and semantic segmentation	[94-97]
Graph	Classification	MPs, spectral, spatial, elevation, and morphological	Generalized graph-based fusion method, semi supervised graph-based (feature) fusion, feature fusion, and decision fusion	[98-100]
Kernel	Urban and complex scene classification	spectral, spatial, height, elevation, morphological, intensity, HFs, MPs, and nDSM	Generalized composite kernel strategy, MKL, HF-MKL, MCKs, KELM-CK, and HySURE-MCKs	[101-103]
Statistical	Urban area, land cover classification, classification of complex forest areas, and geospatial image classification	DSM, DTM, geometric, elevation, spectral, intensity, statistical, and structure	EC-MRF, texture feature extraction based on GLCM, Minimum noise fraction based dimension reduction, ML classfier, GML-LOOC, IGMM, and IGMM-LOGP	[104-107]
Ensemble	Urban land use land cover and local climate zone classification and wetland mapping	DSM, DEM, NDVI, NDMI, morphological, texture, contrast, MNF, and CHM	RF, GBM ensemble based classifier, CNN, linearity preserving projection, unsupervised graph fusion, canonical correlation forest, and rotation forest	[36, 108-110]
Convolutional	Classification and semantic segmentation problem	APs, EPs, MPs, EMAP, EMEP, MEP, DSM, CHM, spatial, elevation, and invariant	Deep convolutional architecture, deep learning, graph-based feature fusion, DNN, 3D-CNN, logistic regression, and deep DF classifier	[111-114]
Hybrid	Urban land use classification	DSM, DEM, intensity, height, nDSM, NDVI, texture measures, and spatial attributes	Pixel and object-based classifier, SVM, MLC, and object-based classfier	[115]
Filter	Land cover land use classification	DSM, DEM, DTM, NDWI, and shadow invariant 1-D feature	multimodal architecture and polinomial fitting-based DEM feature extraction	[116]

filter-based classification of HS-SAR data fusion are summarized in Table 18.

6. Discussion

In this study, we propose a taxonomy of data fusion of HS-LiDAR and HS-SAR based on utilized approaches and summarize the faced challenges. This allows new perspectives on current approaches. In this part of this paper, we summarize significant points of each approach as a guide for future researches. Each approach is categorized in terms of tackled problem and used features of HS-LiDAR and HS-SAR data fusion in Table 19 and Table 20, respectively. We can see that all these conclusion tables give complementary information that can improve the classification performance results. This also means that the classification results could be improved by using multimodal data fusion, particularly this review paper is focused on HS-LiDAR and HS-SAR data fusion.

In this part, we provide brief summary tables of our findings and discuss the results:

7. Conclusion

In this research field, a comprehensive literature overview is performed for the multisource data fusion approaches of HS-LiDAR and HS-SAR images. First, some brief explanations about HS, LiDAR, and SAR have been introduced with the application areas. In addition, application areas and some problems are summarized to perform data fusion between HS LiDAR and SAR data. We also give available datasets that presented the scientific results of the IEEE GRSS Data Fusion Contest, organized by the IEEE GRSS IADF TC between 2006 and 2019. We describe the datasets and the aims in Table 1. These data descriptions are very useful and important for the authors who conduct further studies on the HS LiDAR and SAR data fusion. Then, according to the utilized method, HS LiDAR and SAR data fusion studies were categorized. In addition, many helpful strategies are identified with conclusion tables.

Table 20
Synthesize tables for HS-SAR data fusion

Method	Tackled Problem	Features	Approach	Ref.
Feature	Land cover classfication, forest management, and terrain mapping	EPs, DEMs, polarimetric, tree high canopy cover, timber volume, and 3 polarimetries (HH/HV/VV), eigenvalue, eigenvector, terrain, and textural	Feature-level fusion, decision-level fusion, and parallel feature combination strategy, fuzzy-set theory, SDA, LASSO regression, principal components, feature fusion, and Dempster-Shafer evidence theory	[10, 121-124]
Object	Land use classification and dwelling detection in refugee camps	HH/HV, derived probability features, structure, material, and dwelling density	NCUT, segmentation, feature selection, and rule-based selection	[125-126]
Pixel	Land cover classification and analyzing the impact of the oil spill	Regularization parameter C, kernel, HH/HV/VV, and GLCM features	GA-SVM Algorthm, PCA, SVM, and pixel-level fusion	[128-129]
Kernel	Mines detection	Mean covariance,	Kernel-RX Algorithm	[130-131]
Convolutional	Land cover and forest categorization, image mining, and pansharpening	Optical, polarimetric, correlation, semantic, local-primitive, HH/HV, entropy, mean, eigenvalue, context, contour, curvature, geometric, texture, and subband features	pLSA, LDA, HMpLSA, Deep CNN, Neural Fusion methods, GLM, Adaptive Neural Network, PCNN, and Bayesian	[127, 132-137]
Filter	Speckle reduction method and Forest information extraction	Radiometric, textural, covariance, eigenvalue, Quad-pol feature, DEM, DSM, DCM, stem density, crown-closure, and height	MNF transformation, CSAM, Jong-Sen Lee Algorithm, and Shane Cloude Decomposition	[138-139]

Ideas and approaches deriving from computer vision and machine learning need to be enhanced.

In future studies, we will plan to do a detailed review about DNN architecture with multimodal data fusion. Future directions should include machine learning-based approaches such as deep learning-based approaches.

Declaration of Competing Interest

The authors declare no conflicts of interest.

ACKNOWLEDGMENTS

This work was started and improved during my stay at GIPSA-Lab, France, funded by TUBITAK, grant number 2214/A - International Doctoral Research Fellowship Grand Program. The authors would like to thank Prof. Jocelyn Chanussot for his help and support during his stay. This study has been finalized and funded by Istanbul Gelişim University Scientific Research Projects Application and Research Center. Project number: BP-070220-SK.

References

1 Zhang, J. (2010). Multi-source remote sensing data fusion: status and trends. *International Journal of Image and Data Fusion, 1*(1), 5–24.
2 Dalla Mura, M., et al. (2015). Challenges and opportunities of multimodality and data fusion in remote sensing. *Proceedings of the IEEE, 103*(9), 1585–1601.
3 Klemas, V. V. (2014). Advances in coastal wetland remote sensing. In *2014 IEEE/OES Baltic International Symposium (BALTIC)*. IEEE.
4 Man, Q., et al. (2014). Light detection and ranging and hyperspectral data for estimation of forest biomass: a review. *Journal of Applied Remote Sensing, 8*(1), Article 081598.
5 Gómez-Chova, L., et al. (2015). Multimodal classification of remote sensing images: A review and future directions. *Proceedings of the IEEE, 103*(9), 1560–1584.
6 Wu, B., & Tang, S. (2015). Review of geometric fusion of remote sensing imagery and laser scanning data. *International journal of image and data fusion, 6*(2), 97–114.
7 Bioucas-Dias, J. M., et al. (2012). Hyperspectral unmixing overview: Geometrical, statistical, and sparse regression-based approaches. *IEEE journal of selected topics in applied earth observations and remote sensing, 5*(2), 354–379.
8 Zhang, R., & Ma, J. (2009). Feature selection for hyperspectral data based on recursive support vector machines. *International Journal of Remote Sensing, 30*(14), 3669–3677.
9 Li, S., et al. (2011). An effective feature selection method for hyperspectral image classification based on genetic algorithm and support vector machine. *Knowledge-Based Systems, 24*(1), 40–48.
10 Chouinard, P., & Kerekes, J. (2006). Decision fusion of hyperspectral and SAR data for trafficability assessment. In *2006 IEEE International Symposium on Geoscience and Remote Sensing*. IEEE.
11 Dalla Mura, M., et al. (2010). Morphological attribute profiles for the analysis of very high resolution images. *IEEE Transactions on Geoscience and Remote Sensing, 48*(10), 3747–3762.
12 Ghamisi, P., Benediktsson, J. A., & Sveinsson, J. R. (2013). Automatic spectral–spatial classification framework based on attribute profiles and supervised feature extraction. *IEEE Transactions on Geoscience and Remote Sensing, 52*(9), 5771–5782.
13 Luo, R., et al. (2016). Classification of cloudy hyperspectral image and LiDAR data based on feature fusion AND decision fusion. In *2016 IEEE International Geoscience and Remote Sensing Symposium (IGARSS)*. IEEE.
14 Ghamisi, P., et al. (2016). Extinction profiles for the classification of remote sensing data. *IEEE Transactions on Geoscience and Remote Sensing, 54*(10), 5631–5645.
15 Ghamisi, P., et al. (2016). Hyperspectral data classification using extended extinction profiles. *IEEE Geoscience and Remote Sensing Letters, 13*(11), 1641–1645.
16 Jung, J., et al. (2014). A framework for land cover classification using discrete return LiDAR data: Adopting pseudo-waveform and hierarchical segmentation. *IEEE Journal of Selected Topics in Applied Earth Observations and Remote Sensing, 7*(2), 491–502.
17 Jensen, J. R., & Im, J. (2007). *Remote sensing change detection in urban environments, in Geo-spatial technologies in urban environments* (pp. 7–31). Springer.
18 Madhok, V., & Landgrebe, D. (1999). Supplementing hyperspectral data with digital elevation. In *IEEE 1999 International Geoscience and Remote Sensing Symposium. IGARSS'99 (Cat. No. 99CH36293)*. IEEE.
19 Chen, Q. (2007). Airborne lidar data processing and information extraction. *Photogrammetric engineering and remote sensing, 73*(2), 109.
20 Yokoya, N., Ghamisi, P., & Xia, J. (2017). Multimodal, multitemporal, and multisource global data fusion for local climate zones classification based on ensemble learning. In *2017 IEEE International Geoscience and Remote Sensing Symposium (IGARSS*. IEEE.
21 Pan, Z., et al. (2016). Fusion of LiDAR orthowaveforms and hyperspectral imagery for shallow river bathymetry and turbidity estimation. *IEEE Transactions on Geoscience and Remote Sensing, 54*(7), 4165–4177.
22 Pesaresi, M., & Benediktsson, J. A. (2001). A new approach for the morphological segmentation of high-resolution satellite imagery. *IEEE transactions on Geoscience and Remote Sensing, 39*(2), 309–320.
23 Le Moigne, J., et al. (2002). Multiple sensor image registration, image fusion and dimension reduction of earth science imagery. In *Proceedings of the Fifth International Conference on Information Fusion. FUSION 2002.* IEEE. IEEE Cat. No. 02EX5997.
24 Gamba, P., & Houshmand, B. (2000). Hyperspectral and IFSAR data for 3D urban characterization. In *IGARSS 2000. IEEE 2000 International Geoscience and Remote Sensing Symposium. Taking the Pulse of the Planet: The Role of Remote Sensing in Managing the Environment. Proceedings (Cat. No. 00CH37120*. IEEE.
25 Moreira, A., et al. (2013). A tutorial on synthetic aperture radar. *IEEE Geoscience and remote sensing magazine, 1*(1), 6–43.
26 Franke, J., et al. (2009). Hierarchical multiple endmember spectral mixture analysis (MESMA) of hyperspectral imagery for urban environments. *Remote Sensing of Environment, 113*(8), 1712–1723.

27 Chen, Y., et al. (2009). Hierarchical object oriented classification using very high resolution imagery and LIDAR data over urban areas. *Advances in Space Research, 43*(7), 1101–1110.
28 Jensen, J. R., & Cowen, D. C. (1999). Remote sensing of urban/suburban infrastructure and socio-economic attributes. *Photogrammetric engineering and remote sensing, 65*, 611–622.
29 Powell, R. L., et al. (2007). Sub-pixel mapping of urban land cover using multiple endmember spectral mixture analysis: Manaus, Brazil. *Remote Sensing of environment, 106*(2), 253–267.
30 Gamba, P., Dell'Acqua, F., & Dasarathy, B. V. (2005). Urban remote sensing using multiple data sets: Past, present, and future. *Information Fusion, 6*(4), 319–326.
31 Sankey, T., et al. (2017). UAV lidar and hyperspectral fusion for forest monitoring in the southwestern USA. *Remote Sensing of Environment, 195*, 30–43.
32 Marcus, W. A., & Fonstad, M. A. (2008). Optical remote mapping of rivers at sub-meter resolutions and watershed extents. *Earth Surface Processes and Landforms: The Journal of the British Geomorphological Research Group, 33*(1), 4–24.
33 Allouis, T., et al. (2010). Comparison of LiDAR waveform processing methods for very shallow water bathymetry using Raman, near-infrared and green signals. *Earth Surface Processes and Landforms: The Journal of the British Geomorphological Research Group, 35*(6), 640–650.
34 Koetz, B., et al. (2008). Multi-source land cover classification for forest fire management based on imaging spectrometry and LiDAR data. *Forest Ecology and Management, 256*(3), 263–271.
35 Matsuki, T., Yokoya, N., & Iwasaki, A. (2015). Hyperspectral tree species classification of Japanese complex mixed forest with the aid of LiDAR data. *IEEE Journal of Selected Topics in Applied Earth Observations and Remote Sensing, 8*(5), 2177–2187.
36 Du, Y., et al. (2018). Evaluation on Spaceborne Multispectral Images, Airborne Hyperspectral, and LiDAR Data for Extracting Spatial Distribution and Estimating Aboveground Biomass of Wetland Vegetation Suaeda salsa. *IEEE Journal of Selected Topics in Applied Earth Observations and Remote Sensing, 12*(1), 200–209.
37 Franklin, S. E. (2001). *Remote sensing for sustainable forest management*. CRC press.
38 Gulbe, L., & Mednieks, I. (2013). *Automatic identification of individual tree crowns in mixed forests using fusion of lidar and multispectral data*.
39 Dalponte, M., Bruzzone, L., & Gianelle, D. (2009). Fusion of hyperspectral and LIDAR remote sensing data for the estimation of tree stem diameters. In *2009 IEEE International Geoscience and Remote Sensing Symposium*. IEEE.
40 Van Coillie, F. M., et al. (2015). Optimized feature fusion of LiDAR and hyperspectral data for tree species mapping in closed forest canopies. In *2015 7th Workshop on Hyperspectral Image and Signal Processing: Evolution in Remote Sensing (WHISPERS)*. IEEE.
41 Pham, T. D., et al. (2019). Remote sensing approaches for monitoring mangrove species, structure, and biomass: Opportunities and challenges. *Remote Sensing, 11*(3), 230.
42 Bioucas-Dias, J. M., et al. (2013). Hyperspectral remote sensing data analysis and future challenges. *IEEE Geoscience and remote sensing magazine, 1*(2), 6–36.
43 Ghamisi, P., Benediktsson, J. A., & Phinn, S. (2015). Land-cover classification using both hyperspectral and LiDAR data. *International Journal of Image and Data Fusion, 6*(3), 189–215.
44 Eismann, M. T. (2006). Strategies for hyperspectral target detection in complex background environments. In *2006 IEEE Aerospace Conference*. IEEE.
45 Zhang, Q., et al. (2013). Detecting objects under shadows by fusion of hyperspectral and lidar data: A physical model approach. In *2013 5th Workshop on Hyperspectral Image and Signal Processing: Evolution in Remote Sensing (WHISPERS)*. IEEE.
46 Zhu, Z., & Woodcock, C. E. (2014). Automated cloud, cloud shadow, and snow detection in multitemporal Landsat data: An algorithm designed specifically for monitoring land cover change. *Remote Sensing of Environment, 152*, 217–234.
47 Luo, R., et al. (2017). Fusion of hyperspectral and LiDAR data for classification of cloud-shadow mixed remote sensed scene. *IEEE Journal of Selected Topics in Applied Earth Observations and Remote Sensing, 10*(8), 3768–3781.
48 Rasti, B., et al. (2017). Fusion of hyperspectral and LiDAR data using sparse and low-rank component analysis. *IEEE Transactions on Geoscience and Remote Sensing, 55*(11), 6354–6365.
49 Samawi, V. W., & Basheer, O. A. A. (2008). The effect of features reduction on different texture classifiers. In *2008 3rd IEEE Conference on Industrial Electronics and Applications*. IEEE.
50 Kumar, S., Ghosh, J., & Crawford, M. M. (2001). Best-bases feature extraction algorithms for classification of hyperspectral data. *IEEE Transactions on Geoscience and remote sensing, 39*(7), 1368–1379.
51 Jimenez, L. O., & Landgrebe, D. A. (1999). Hyperspectral data analysis and supervised feature reduction via projection pursuit. *IEEE Transactions on Geoscience and Remote Sensing, 37*(6), 2653–2667.
52 Fauvel, M., Chanussot, J., & Benediktsson, J. A. (2009). Kernel principal component analysis for the classification of hyperspectral remote sensing data over urban areas. *EURASIP Journal on Advances in Signal Processing, 2009*(1), Article 783194.
53 Ghamisi, P., & Benediktsson, J. A. (2014). Feature selection based on hybridization of genetic algorithm and particle swarm optimization. *IEEE Geoscience and remote sensing letters, 12*(2), 309–313.
54 Alparone, L., et al. (2007). Comparison of pansharpening algorithms: Outcome of the 2006 GRS-S data-fusion contest. *IEEE Transactions on Geoscience and Remote Sensing, 45*(10), 3012–3021.
55 Pacifici, F., et al. (2008). Urban mapping using coarse SAR and optical data: Outcome of the 2007 GRSS data fusion contest. *IEEE Geoscience and Remote Sensing Letters, 5*(3), 331–335.
56 Licciardi, G., et al. (2009). Decision fusion for the classification of hyperspectral data: Outcome of the 2008 GRS-S data fusion contest. *IEEE Transactions on Geoscience and Remote Sensing, 47*(11), 3857–3865.
57 Longbotham, N., et al. (2012). Multi-modal change detection, application to the detection of flooded areas: Outcome of the 2009–2010 data fusion contest. *IEEE Journal of selected topics in applied earth observations and remote sensing, 5*(1), 331–342.
58 Pacifici, F., & Du, Q. (2012). Foreword to the special issue on optical multiangular data exploitation and outcome of the 2011 GRSS data fusion contest. In *IEEE-INST ELECTRICAL ELECTRONICS ENGINEERS INC 445 HOES LANE, PISCATAWAY, NJ*.
59 Berger, C., et al. (2013). Multi-modal and multi-temporal data fusion: Outcome of the 2012 GRSS data fusion contest. *IEEE Journal of Selected Topics in Applied Earth Observations and Remote Sensing, 6*(3), 1324–1340.
60 Debes, C., et al. (2014). Hyperspectral and LiDAR data fusion: Outcome of the 2013 GRSS data fusion contest. *IEEE Journal of Selected Topics in Applied Earth Observations and Remote Sensing, 7*(6), 2405–2418.
61 Liao, W., et al. (2015). Processing of multiresolution thermal hyperspectral and digital color data: Outcome of the 2014 IEEE GRSS data fusion contest. *IEEE Journal of Selected Topics in Applied Earth Observations and Remote Sensing, 8*(6), 2984–2996.
62 Vo, A.-V., et al. (2016). Processing of extremely high resolution LiDAR and RGB data: Outcome of the 2015 IEEE GRSS data fusion contest—Part B: 3-D contest. *IEEE Journal of Selected Topics in Applied Earth Observations and Remote Sensing, 9*(12), 5560–5575.
63 Mou, L., et al. (2017). Multitemporal very high resolution from space: Outcome of the 2016 IEEE GRSS data fusion contest. *IEEE Journal of Selected Topics in Applied Earth Observations and Remote Sensing, 10*(8), 3435–3447.
64 Yokoya, N., et al. (2018). Open data for global multimodal land use classification: Outcome of the 2017 IEEE GRSS Data Fusion Contest. *IEEE Journal of Selected Topics in Applied Earth Observations and Remote Sensing, 11*(5), 1363–1377.
65 Le Saux, B., et al. (2018). 2018 IEEE GRSS Data Fusion Contest: Multimodal land use classification [technical committees]. *IEEE geoscience and remote sensing magazine, 6*(1), 52–54.
66 http, 2021 http://www.grss-ieee.org/community/technicalcommittees/data-fusion/2019-ieee-grss-data-fusion-contest-data/.
67 Hossain, M., et al. (2015). The application of remote sensing to seagrass ecosystems: an overview and future research prospects. *International Journal of Remote Sensing, 36*(1), 61–114.
68 Liao, W., et al. (2017). A comparison on multiple level features for fusion of hyperspectral and LiDAR data. In *2017 Joint Urban Remote Sensing Event (JURSE)*. IEEE.
69 Hasani, H., Samadzadegan, F., & Reinartz, P. (2017). A metaheuristic feature-level fusion strategy in classification of urban area using hyperspectral imagery and LiDAR data. *European Journal of Remote Sensing, 50*(1), 222–236.
70 Khodadadzadeh, M., et al. (2015). Fusion of hyperspectral and LiDAR remote sensing data using multiple feature learning. *IEEE Journal of Selected Topics in Applied Earth Observations and Remote Sensing, 8*(6), 2971–2983.
71 Pedergnana, M., et al. (2012). Classification of remote sensing optical and LiDAR data using extended attribute profiles. *IEEE Journal of Selected Topics in Signal Processing, 6*(7), 856–865.
72 Samiappan, S., Dabbiru, L., & Moorhead, R. (2016). Fusion of hyperspectral and LiDAR data using random feature selection and morphological attribute profiles. In *2016 8th Workshop on Hyperspectral Image and Signal Processing: Evolution in Remote Sensing (WHISPERS)*. IEEE.
73 Priem, F., & Canters, F. (2016). Synergistic use of LiDAR and APEX hyperspectral data for high-resolution urban land cover mapping. *Remote sensing, 8*(10), 787.
74 Rasti, B., Ghamisi, P., & Gloaguen, R. (2017). Hyperspectral and lidar fusion using extinction profiles and total variation component analysis. *IEEE Transactions on Geoscience and Remote Sensing, 55*(7), 3997–4007.
75 Dalponte, M., Frizzera, L., & Gianelle, D. (2014). Fusion of hyperspectral and LiDAR data for forest attributes estimation. In *2014 IEEE Geoscience and Remote Sensing Symposium*. IEEE.
76 Liao, W., et al. (2017). Fusion of multi-scale hyperspectral and lidar features for tree species mapping. In *2017 IEEE International Geoscience and Remote Sensing Symposium (IGARSS*. IEEE.
77 Xu, X., Li, J., & Plaza, A. (2016). Fusion of hyperspectral and LiDAR data using morphological component analysis. In *2016 IEEE International Geoscience and Remote Sensing Symposium (IGARSS)*. IEEE.
78 Bhaskaran, S., Paramananda, S., & Ramnarayan, M. (2010). Per-pixel and object-oriented classification methods for mapping urban features using Ikonos satellite data. *Applied Geography, 30*(4), 650–665.
79 Petropoulos, G. P., Kalaitzidis, C., & Vadrevu, K. P. (2012). Support vector machines and object-based classification for obtaining land-use/cover cartography from Hyperion hyperspectral imagery. *Computers & Geosciences, 41*, 99–107.
80 Sugumaran, R., & Voss, M. (2007). Object-oriented classification of LIDAR-fused hyperspectral imagery for tree species identification in an urban environment. In *2007 Urban Remote Sensing Joint Event*. IEEE.
81 Marpu, P. R., & Martinez, S. S. (2015). Object-based fusion of hyperspectral and LiDAR data for classification of urban areas. In *2015 7th Workshop on Hyperspectral Image and Signal Processing: Evolution in Remote Sensing (WHISPERS)*. IEEE.
82 Kanaev, A., et al. (2011). Object level HSI-LIDAR data fusion for automated detection of difficult targets. *Optics express, 19*(21), 20916–20929.
83 Alonzo, M., Bookhagen, B., & Roberts, D. A. (2014). Urban tree species mapping using hyperspectral and lidar data fusion. *Remote Sensing of Environment, 148*, 70–83.
84 Leonardi, F., Almeida, C. M., Fonseca, L. M. G., Tomás, L. R., & Oliveira, C. G. (2012). Genetic Algorithms and Data Mining Applied to optical orbital and LiDAR

data for object-based classification of Urban Land cover. In *Proceedings of the 4th GEOBIA* (pp. 649–654).
85 Kiani, K., et al. (2014). Urban area object-based classification by fusion of hyperspectral and LiDAR data. In *2014 IEEE Geoscience and Remote Sensing Symposium*. IEEE.
86 Aytaylan, H., & Yuksel, S. E. (2016). Semantic segmentation of hyperspectral images with the fusion of LiDAR data. In *2016 IEEE International Geoscience and Remote Sensing Symposium (IGARSS)*. IEEE.
87 Liu, Y., et al. (2017). Multi-superpixelization-based convex formulation for joint classification of hyperspectral and lidar data. In *2017 IEEE International Geoscience and Remote Sensing Symposium (IGARSS*. IEEE.
88 Castrodad, A., et al. (2012). Sparse modeling for hyperspectral imagery with lidar data fusion for subpixel mapping. In *2012 IEEE International Geoscience and Remote Sensing Symposium*. IEEE.
89 Wang, H., Glennie, C., & Prasad, S. (2013). Voxelization of full waveform LiDAR data for fusion with hyperspectral imagery. In *2013 IEEE International Geoscience and Remote Sensing Symposium-IGARSS*. IEEE.
90 Uezat, T., Fauvel, M., & Dobigeon, N. (2018). Lidar-Driven Spatial Regularization for Hyperspectral Unmixing. In *IGARSS 2018-2018 IEEE International Geoscience and Remote Sensing Symposium*. IEEE.
91 Mahmoudabadi, H., Shoaf, T., & Olsen, M. J. (2013). Superpixel clustering and planar fit segmentation of 3D LIDAR point clouds. In *2013 Fourth International Conference on Computing for Geospatial Research and Application*. IEEE.
92 Puttonen, E., et al. (2015). Artificial target detection with a hyperspectral LiDAR over 26-h measurement. *Optical Engineering, 54*(1), Article 013105.
93 Sadjadi, S. Y., & Parsian, S. (2017). Combining Hyperspectral and LiDAR Data for Building Extraction using Machine Learning Technique. *International Journal of Computers*, (2).
94 Matsuki, T., Yokoya, N., & Iwasaki, A. (2014). Hyperspectral tree species classification with an aid of lidar data. In *2014 6th Workshop on Hyperspectral Image and Signal Processing: Evolution in Remote Sensing (WHISPERS)*. IEEE.
95 Broadwater, J., & Banerjee, A. (2013). Improved atmospheric compensation of hyperspectral imagery using LIDAR. In *2013 IEEE International Geoscience and Remote Sensing Symposium-IGARSS*. IEEE.
96 Lemp, D., & Weidner, U. (2005). Improvements of roof surface classification using hyperspectral and laser scanning data. In *Proc. ISPRS Joint Conf.: 3rd Int. Symp. Remote Sens. Data Fusion Over Urban Areas (URBAN), 5th Int. Symp. Remote Sens. Urban Areas (URS)*.
97 Dechesne, C., et al. (2017). How to combine lidar and very high resolution multispectral images for forest stand segmentation?. In *2017 IEEE International Geoscience and Remote Sensing Symposium (IGARSS*. IEEE.
98 Liao, W., et al. (2014). Generalized graph-based fusion of hyperspectral and LiDAR data using morphological features. *IEEE Geoscience and Remote Sensing Letters, 12*(3), 552–556.
99 Liao, W., et al. (2014). Combining feature fusion and decision fusion for classification of hyperspectral and LiDAR data. In *2014 IEEE Geoscience and Remote Sensing Symposium*. IEEE.
100 Liao, W., et al. (2015). Semi-supervised graph fusion of hyperspectral and LiDAR data for classification. In *2015 IEEE International Geoscience and Remote Sensing Symposium (IGARSS)*. IEEE.
101 Khodadadzadeh, M., et al. (2015). Fusion of hyperspectral and lidar data using generalized composite kernels: A case study in Extremadura, Spain. In *2015 IEEE International Geoscience and Remote Sensing Symposium (IGARSS)*. IEEE.
102 Ghamisi, P., Rasti, B., & Benediktsson, J. A. (2018). Multisensor Composite Kernels Based on Extreme Learning Machines. *IEEE Geoscience and Remote Sensing Letters, 16*(2), 196–200.
103 Gu, Y., et al. (2015). A novel MKL model of integrating LiDAR data and MSI for urban area classification. *IEEE transactions on geoscience and remote sensing, 53*(10), 5312–5326.
104 Ni, L., et al. (2014). Edge-constrained Markov random field classification by integrating hyperspectral image with LiDAR data over urban areas. *Journal of Applied Remote Sensing, 8*(1), Article 085089.
105 Abbasi, B., et al. (2015). Fusion of hyperspectral and lidar data based on dimension reduction and maximum likelihood. *The International Archives of Photogrammetry, Remote Sensing and Spatial Information Sciences, 40*(7), 569.
106 Dalponte, M., Bruzzone, L., & Gianelle, D. (2008). Fusion of hyperspectral and LIDAR remote sensing data for classification of complex forest areas. *IEEE Transactions on Geoscience and Remote Sensing, 46*(5), 1416–1427.
107 Wu, H., & Prasad, S. (2013). Infinite Gaussian mixture models for robust decision fusion of hyperspectral imagery and full waveform LiDAR data. In *2013 IEEE Global Conference on Signal and Information Processing*. IEEE.
108 Sukhanov, S., et al. (2018). Fusion of Lidar, Hyperspectral and RGB Data for Urban Land Use and Land Cover Classification. In *IGARSS 2018-2018 IEEE International Geoscience and Remote Sensing Symposium*. IEEE.
109 Sukhanov, S., et al. (2017). Multilevel ensembling for local climate zones classification. In *2017 IEEE International Geoscience and Remote Sensing Symposium (IGARSS*. IEEE.
110 Xia, J., Yokoya, N., & Iwasaki, A. (2018). Fusion of hyperspectral and lidar data with a novel ensemble classifier. *IEEE Geoscience and Remote Sensing Letters, 15*(6), 957–961.
111 Salman, M., & Yüksel, S. E. (2018). Fusion of hyperspectral image and LiDAR data and classification using deep convolutional neural networks. In *2018 26th Signal Processing and Communications Applications Conference (SIU)*. IEEE.
112 Ghamisi, P., Höfle, B., & Zhu, X. X. (2016). Hyperspectral and LiDAR data fusion using extinction profiles and deep convolutional neural network. *IEEE Journal of Selected Topics in Applied Earth Observations and Remote Sensing, 10*(6), 3011–3024.
113 Chen, Y., et al. (2016). Deep fusion of hyperspectral and LiDAR data for thematic classification. In *2016 IEEE International Geoscience and Remote Sensing Symposium (IGARSS)*. IEEE.
114 Xia, J., Ming, Z., & Iwasaki, A. (2018). Multiple sources data fusion via deep forest. In *IGARSS 2018-2018 IEEE International Geoscience and Remote Sensing Symposium*. IEEE.
115 Man, Q., Dong, P., & Guo, H. (2015). Pixel-and feature-level fusion of hyperspectral and lidar data for urban land-use classification. *International Journal of Remote Sensing, 36*(6), 1618–1644.
116 Demirkesen, C., Teke, M., & Sakarya, U. (2014). Hyperspectral images and lidar based DEM fusion: A multi-modal landuse classification strategy. In *2014 IEEE Geoscience and Remote Sensing Symposium*. IEEE.
117 Bhogall, A., et al. (2001). Extraction of forest attribute information using multisensor data fusion techniques: A case study for a test site on Vancouver island, British Columbia. In *2001 IEEE Pacific Rim Conference on Communications, Computers and Signal Processing (IEEE Cat. No. 01CH37233)*. IEEE.
118 Zhang, H., Lin, H., & Li, Y. (2015). Impacts of feature normalization on optical and SAR data fusion for land use/land cover classification. *IEEE Geoscience and Remote Sensing Letters, 12*(5), 1061–1065.
119 Pohl, C., & Van Genderen, J. L. (1998). Review article multisensor image fusion in remote sensing: concepts, methods and applications. *International journal of remote sensing, 19*(5), 823–854.
120 Huang, H.-Y., & Kuo, B.-C. (2010). Double nearest proportion feature extraction for hyperspectral-image classification. *IEEE Transactions on Geoscience and Remote Sensing, 48*(11), 4034–4046.
121 Li, T., et al. (2013). Classification-oriented hyperspectral and PolSAR images synergic processing. In *2013 IEEE International Geoscience and Remote Sensing Symposium-IGARSS*. IEEE.
122 Yoshida, K., et al. (2011). A methodology of forest monitoring from hyperspectral images with sparse regularization. In *2011 IEEE International Geoscience and Remote Sensing Symposium*. IEEE.
123 Chouinard, P., & Kerekes, J. (2006). Decision Fusion of Hyperspectral and SAR Data for Trafficability Assessment. In *IEEE International Symposium on Geoscience and Remote Sensing*. IEEE.
124 Jouan, A., Allard, Y., & Allen, S. (2002). *Land Use Mapping with Evidential Fusion of Polarimetric Synthetic Aperture Radar and Hyperspectral Imagery*. LOCKHEED MARTIN CANADA MONTREAL (QUEBEC).
125 Hu, J., et al. (2016). Object based fusion of polarimetric SAR and hyperspectral imaging for land use classification. In *2016 8th Workshop on Hyperspectral Image and Signal Processing: Evolution in Remote Sensing (WHISPERS)*. IEEE.
126 Spröhnle, K., Fuchs, E.-M., & Pelizari, P. A. (2017). Object-based analysis and fusion of optical and SAR satellite data for dwelling detection in refugee camps. *IEEE Journal of Selected Topics in Applied Earth Observations and Remote Sensing, 10*(5), 1780–1791.
127 Fernandez-Beltran, R., et al. (2018). Multimodal probabilistic latent semantic analysis for sentinel-1 and sentinel-2 image fusion. *IEEE Geoscience and Remote Sensing Letters, 15*(9), 1347–1351.
128 Sukawattanavijit, C., Chen, J., & Zhang, H. (2017). GA-SVM algorithm for improving land-cover classification using SAR and optical remote sensing data. *IEEE Geoscience and Remote Sensing Letters, 14*(3), 284–288.
129 Dabbiru, L., et al. (2015). Fusion of synthetic aperture radar and hyperspectral imagery to detect impacts of oil spill in Gulf of Mexico. In *2015 IEEE international geoscience and remote sensing symposium (IGARSS)*. IEEE.
130 Nasrabadi, N. M. (2008). A nonlinear kernel-based joint fusion/detection of anomalies using hyperspectral and SAR imagery. In *2008 15th IEEE International Conference on Image Processing*. IEEE.
131 Nasrabadi, N. M. (2008). Multisensor joint fusion and detection of mines using SAR and Hyperspectral. *SENSORS*, 1056–1059.
132 Fernandez-Beltran, R., et al. (2018). Remote sensing image fusion using hierarchical multimodal probabilistic latent semantic analysis. *IEEE Journal of Selected Topics in Applied Earth Observations and Remote Sensing, 11*(12), 4982–4993.
133 Hu, J., et al. (2017). FusioNet: A two-stream convolutional neural network for urban scene classification using PolSAR and hyperspectral data. In *2017 Joint Urban Remote Sensing Event (JURSE)*. IEEE.
134 Chiarella, M., et al. (2003). Multisensor image fusion and mining: from neural systems to COTS software with application to remote sensing AFE. In *IEEE Workshop on Advances in Techniques for Analysis of Remotely Sensed Data, 2003*. IEEE.
135 Volden, E., Solberg, A. S., & Huseby, R. B. (1998). Forest classification using spectrometer and SAR data. in IGARSS'98. Sensing and Managing the Environment. In *1998 IEEE International Geoscience and Remote Sensing. Symposium Proceedings. (Cat. No. 98CH36174)*. IEEE.
136 Wang, X., et al. (2019). The PAN and MS Image Pansharpening Algorithm Based on Adaptive Neural Network and Sparse Representation in the NSST Domain. *IEEE Access, 7*, 52508–52521.
137 Solberg, A. H. S., Jain, A. K., & Taxt, T. (1994). Multisource classification of remotely sensed data: fusion of Landsat TM and SAR images. *IEEE transactions on Geoscience and Remote Sensing, 32*(4), 768–778.
138 Zhou, Q., Gong, P., & Guo, Z. (2010). A speckle reduction method based on hyperspectral and SAR image fusion. In *2010 International Conference on Multimedia Technology*. IEEE.
139 Goodenough, D. G., et al. (2008). Data fusion study between polarimetric SAR, hyperspectral and LiDAR data for forest information. In *IGARSS 2008-2008 IEEE International Geoscience and Remote Sensing Symposium*. IEEE.
140 Zhang, M., Li, W., Wei, X., & Li, X. (2018). Collaborative Classification of Hyperspectral and LIDAR Data Using Unsupervised Image-to-Image CNN. In *10th IAPR Workshop on Pattern Recognition in Remote Sensing (PRRS)*.

141 Wang, J., Zhang, J., Guo, Q., & Li, T (2019). Fusion of Hyperspectral and Lidar Data Based On Dual-Branch Convolutional Neural Network. In *IEEE International Geoscience and Remote Sensing Symposium*.
142 Chen, C., Zhao, X., Li, W., Tao, R., & Du, Q. (2019). Collaborative Classification of Hyperspectral and Lidar Data With Information Fusion and Deep Nets. In *IEEE International Geoscience and Remote Sensing Symposium*.
143 Morchhale, S., Pauca, V. P., Plemmons, R. J., & Torgersen, T. C. (2016). Classification of pixel-level fused hyperspectral and lidar data using deep convolutional neural networks. In *8th Workshop on Hyperspectral Image and Signal Processing: Evolution in Remote Sensing (WHISPERS)*.
144 Liao, W., Coillie, F. V., Gao, L., Li, L., Zhang, B., & Chanussot, J. (2018). Deep Learning for Fusion of APEX Hyperspectral and Full-Waveform LiDAR Remote Sensing Data for Tree Species Mapping. *IEEE Access*.
145 Xu, Y., Du, B., & Zhang, L. (2018). Multi-Source Remote Sensing Data Classification via Fully Convolutional Networks and Post-Classification Processing. In *IEEE International Geoscience and Remote Sensing Symposium*.